JOURNAL OF NEUROPHYSIOLOGY
Vol. 62, No. 3, September 1989. Printed in U.S.A.

# Human Cortical Potentials Evoked by Stimulation of the Median Nerve. I. Cytoarchitectonic Areas Generating Short-Latency Activity

TRUETT ALLISON, GREGORY McCARTHY, CHARLES C. WOOD, TERRANCE M. DARCEY, DENNIS D. SPENCER, AND PETER D. WILLIAMSON

*Neuropsychology Laboratory, Veterans Administration Medical Center, West Haven, 06516; and Department of Neurology and Section of Neurosurgery, Yale University School of Medicine, New Haven, Connecticut 06520*

## SUMMARY AND CONCLUSIONS

*1.* The anatomic generators of human somatosensory evoked potentials (SEPs) in the 20 to 40-ms latency range were investigated by means of cortical surface and transcortical recordings during neurosurgery and recordings from chronically implanted depth probes in epileptic patients.

*2.* Three groups of SEPs evoked by median nerve stimulation were recorded from the hand representation area of sensorimotor cortex: P20–N30, recorded anterior to the central sulcus (CS); N20–P30, recorded posterior to the CS; and P25–N35, recorded near and on either side of the CS. These potentials were similar in morphology and surface distribution whether the patient was operated under local or general anesthesia and were evoked only by contralateral stimulation; stimulation of the ipsilateral median nerve produced no detectable activity in the 20 to 40-ms latency range.

*3.* P20–N30 and N20–P30 exhibited polarity inversions across the CS but were similar in polarity and morphology on the cortical surface and in the white matter. Together with anatomic considerations, these spatial distributions strongly suggest that **P20–N30 and N20–P30 are** recordings from the "surface" and "white matter" sides of a tangentially oriented generator located in the posterior wall of the **CS in *area 3b* of somatosensory cortex.**

*4.* P25–N35 was largest in the medial portion of the hand area of somatosensory cortex and did not show polarity inversion across the CS. Our transcortical recordings did not clarify its origin, but its spatial distribution and comparison with the transcortical recordings of Goldring et al. 1970; Kelly et al. 1965; Stohr and Goldring 1969 strongly suggest that P25–N35 is produced by a radially oriented generator located in the anterior crown of the postcentral gyrus in *area 1* of somatosensory cortex, in a region ~1 cm medial to the region of largest *area 3b* potentials.

*5.* **Later P25-like potentials were sometimes recorded near the CS, lateral to the region from which the largest P25 was recorded. These potentials appear to reflect the activation of more lateral regions of the hand representation of *area 1* than those responsible for P25.**

*6.* P20–N30 and P25–N35 are thought to be equivalent to the primary evoked response recorded from somatosensory cortex of other mammals, particularly Old World monkeys having a geometric and cytoarchitectonic organization of somatosensory cortex similar to that of humans.

*7.* The major spatial and temporal features of SEPs recorded from the surface of human sensorimotor cortex are well accounted for by a model having two generators with different timecourses and with fixed locations and orientations in cytoarchitectonic *areas 3b* and *1*.

## INTRODUCTION

The anatomic generators of human somatosensory evoked potentials (SEPs) in the 20 to 40-ms latency range have been the subject of considerable debate (Allison et al. 1980, 1982; Broughton et al. 1969, 1981; Celesia 1979; Chiappa 1983; Deiber et al. 1986; Desmedt et al. 1981, 1985; DeWeerd et al. 1985; Jones and Power 1984; Lueders et al. 1983; Mauguière et al. 1983; Papakostopoulos and Crow 1984; Slimp et al. 1986; Stohr and Goldring 1969; Wood et al. 1985; Yamada et al. 1984). Although there is agreement that some portion of the spatiotemporal SEP distribution originates in somatosensory cortex, there is disagreement about the specific regions involved and whether any SEPs originate in motor cortex. In this paper we address these questions by the use of SEPs derived from cortical surface, transcortical, and depth probe recordings in patients undergoing neurosurgical procedures. The generators of long-latency SEPs are considered in the following paper (Allison et al. 1989).

One important type of evidence concerning the generators of extracellular potentials such as SEPs is the three-dimensional distribution of potential on the cortical surface and within the brain, which permits the locations of transmembrane current flow to be determined (Mitzdorf 1985). Although such data with adequate spatial resolution cannot be obtained in humans, the locations of cortical generators can be determined at a more macroscopic level by assessing the polarity and gradient of potentials recorded from the cortical surface and white matter. A polarity inversion and sharp potential gradient from surface to white matter are regarded as providing strong evidence that the potentials are generated in cortex between or adjacent to the recording electrodes. Conversely, similar waveforms and shallow gradients between surface and white matter suggest that the activity is generated at more distant sites (Dykes 1978; Goldring et al. 1970; Landau 1967; Schlag 1973; Wood and Allison 1981). Thus, in the present study, we attempted to determine the distribution, waveform, and spatial gradient of potentials recorded on the surface of sensorimotor cortex and within the central sulcus and white matter. In addition, a large body of work describing potentials evoked in somatosensory cortex of nonhuman primates (Allison et al. 1986; Arezzo et al. 1979, 1981; Gardner et al. 1984; Goldring et al. 1970; Kulics and





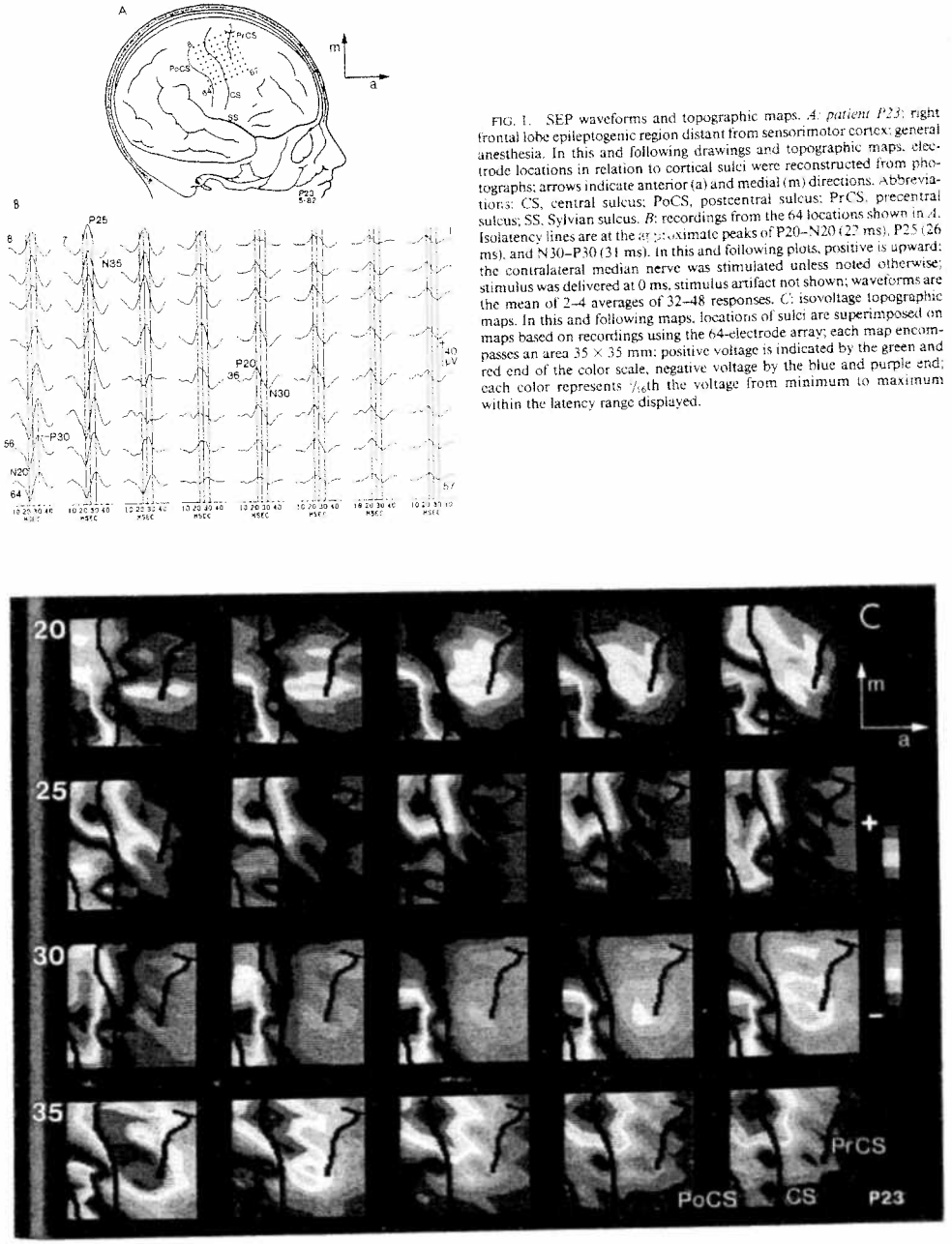


FIG. 1. SEP waveforms and topographic maps. *A*: *patient P23*; right frontal lobe epileptogenic region distant from sensorimotor cortex; general anesthesia. In this and following drawings and topographic maps, electrode locations in relation to cortical sulci were reconstructed from photographs; arrows indicate anterior (a) and medial (m) directions. Abbreviations: CS, central sulcus; PoCS, postcentral sulcus; PrCS, precentral sulcus; SS, Sylvian sulcus. *B*: recordings from the 64 locations shown in *A*. Isolatency lines are at the approximate peaks of P20–N20 (22 ms), P25 (26 ms), and N30–P30 (31 ms). In this and following plots, positive is upward; the contralateral median nerve was stimulated unless noted otherwise; stimulus was delivered at 0 ms, stimulus artifact not shown; waveforms are the mean of 2–4 averages of 32–48 responses. *C*: isovoltage topographic maps. In this and following maps, locations of sulci are superimposed on maps based on recordings using the 64-electrode array; each map encompasses an area 35 × 35 mm; positive voltage is indicated by the green and red end of the color scale, negative voltage by the blue and purple end; each color represents $\frac{1}{16}$th the voltage from minimum to maximum within the latency range displayed.

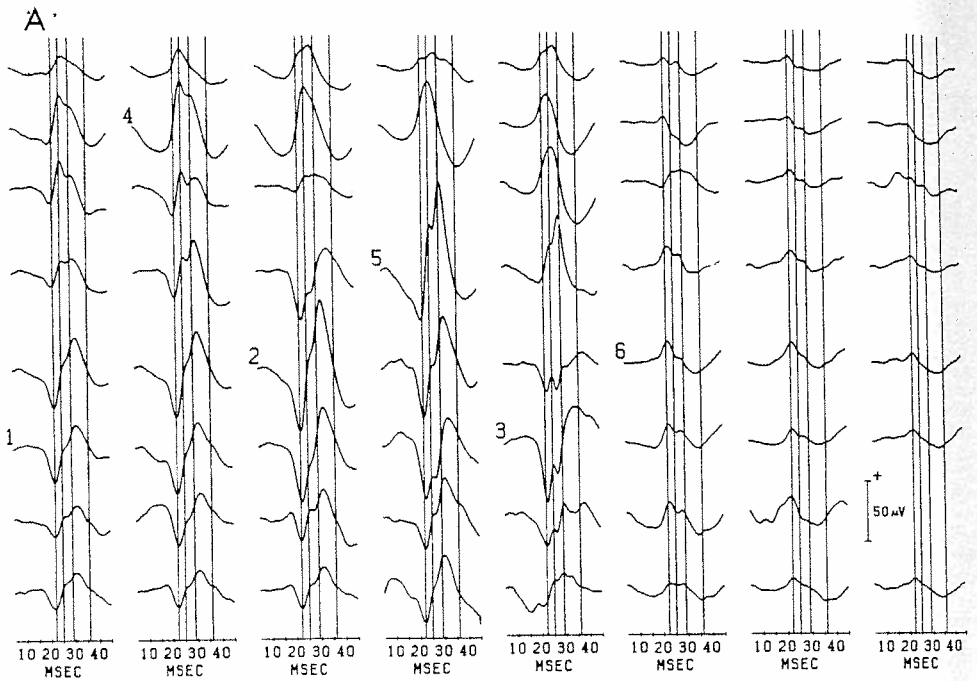


FIG. 2. SEP waveforms and topographic maps. *A: patient K2*; right frontal lobe epileptogenic region distant from sensorimotor cortex; general anesthesia. Array orientation as in Fig. 1. Isolatency lines are at the approximate peaks of P20–N20 (22 ms), P25 (25 ms), P25-like potential (29 ms), and P25-like potential (36 ms). *B*: maps at latencies of isolatency lines in *A*. *C*: waveforms at selected locations shown in *A* and *B*.

Cauller 1986; Zimmerman 1968) and other mammals (Allison et al. 1966, 1980; Dykes 1978; Perl and Whitlock 1955; Schlag 1973; Towe 1966; Werner and Whitsel 1973; Woolsey and Fairman 1946) aided interpretation of the human recordings. Unless noted otherwise, all human and animal potentials discussed in this paper were evoked by electrical stimulation of the contralateral median nerve at the wrist.

## METHODS

Techniques for recording SEPs from the exposed cortical surface, and their use as a method of localizing somatosensory and motor cortex, are described in detail elsewhere (Wood et al. 1988). Briefly, intraoperative recordings from the cortical surface were made in 52 patients operated under local anesthesia or general endotrachael anesthesia for removal of mass lesions or epileptogenic foci. SEPs were recorded either from individually placed silver-ball electrodes or from a 64-electrode array (8 × 8 grid of electrodes with 5-mm interelectrode spacing). The spatial distribution of voltage over the cortical surface was illustrated by isovoltage topographic maps in which amplitudes at locations between recording electrodes were estimated by linear interpolation. In five cases transcortical recordings from sensorimotor cortex were also obtained; electrodes consisted of a 2 mm diam ring (surface electrode) through which a wire exposed for 1 mm at the tip extended to a depth of 6 mm (deep electrode). Recording was to a common reference (linked ears or a needle electrode placed in reflected temporal muscle).

SEPs were also recorded in 12 epileptic patients from 18-contact platinum-iridium depth probes implanted in frontal, temporal, and occipital regions to localize seizure foci (Spencer et al. 1982). Recordings were made several days after probe implantation; patients were awake and unsedated. The common reference was linked ears or balanced sternovertebral electrodes. In some of these patients, cortical surface recordings were obtained during subsequent surgery to remove a seizure focus. Before either type of intracranial recording, scalp recordings were often obtained using a balanced sternovertebral common reference.

For all types of recordings, stimuli were 0.4–2/s, 0.5-ms duration constant-current pulses delivered to the contralateral or ipsilateral median nerve at the wrist at an intensity producing a moderate thumb twitch. Three averages of 32–48 responses (intraoperative recordings) or 128–256 responses (depth-probe and scalp recordings) were typically obtained using a digitizing rate of 2,000 Hz and filter settings of 1–1,000 Hz (−3 dB). The protocols used in this study were approved by the Human Investigation Committees of the West Haven VA Medical Center and Yale University School of Medicine. Informed consent was obtained.



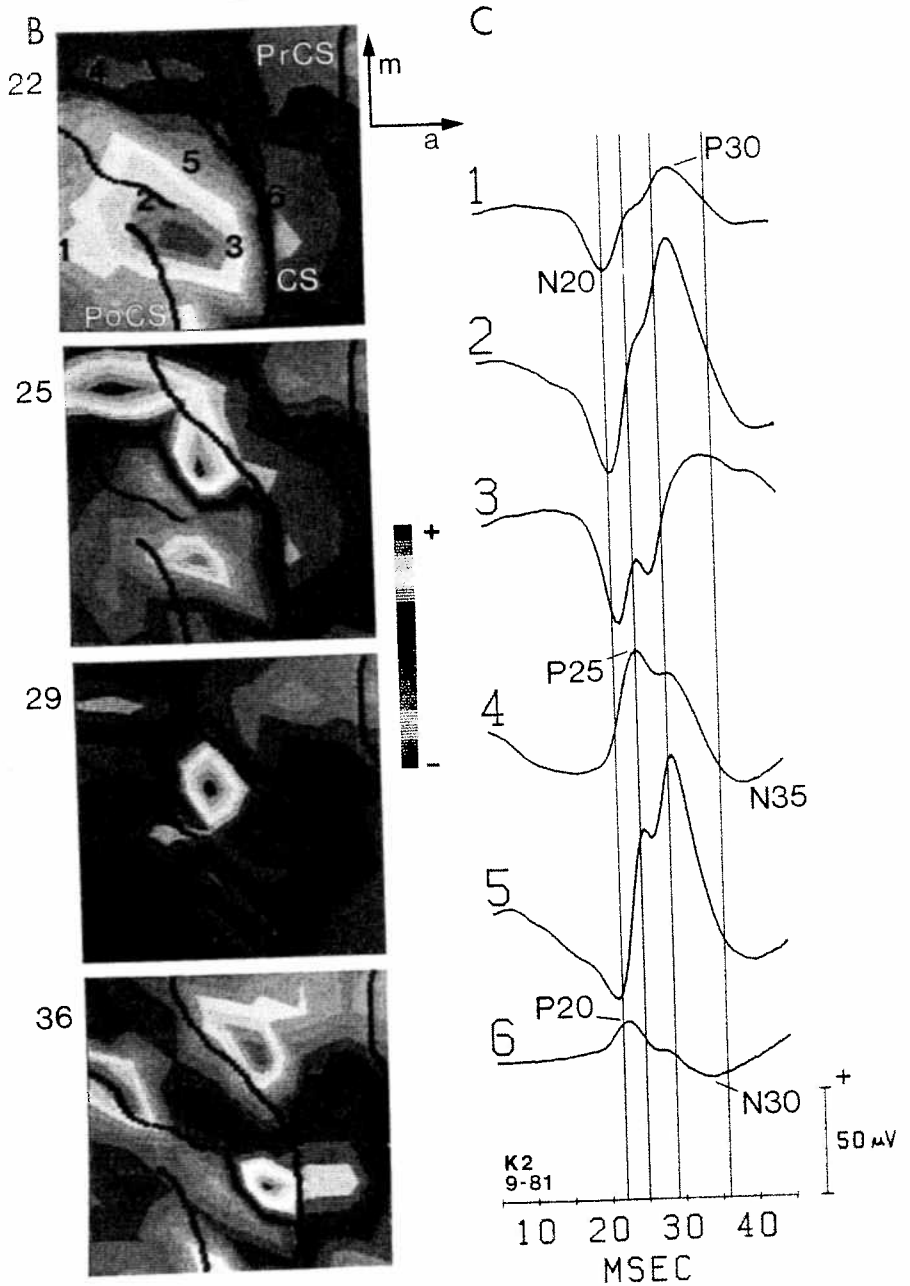


FIG. 2. (*continued*)

TABLE 1. *Short-latency SEPs summarized*

| | Latency or Amplitude | | | | | | | | |
|---|---|---|---|---|---|---|---|---|---|
| | P20 Lat, ms | N30 Lat, ms | P20–N30 Amp, μV | N20 Lat, ms | P30 Lat, ms | N20–P30 Amp, μV | P25 Lat, ms | N35 Lat, ms | P25–N35 Amp, μV |
| Anesthesia | | | | | | | | | |
| Local | 22.1 ± 0.5 (18) | 33.9 ± 1.0 (18) | 98.5 ± 20.8* (18) | 22.3 ± 0.4 (18) | 33.8 ± 1.1 (18) | 134.0 ± 23.4* (18) | 24.8 ± 0.4 (16) | 38.0 ± 0.7 (10) | 195.3 ± 60.9* (10) |
| General | 22.7 ± 0.3 (33) | 33.3 ± 0.5 (33) | 48.3 ± 8.2* (33) | 22.3 ± 0.3 (34) | 31.8 ± 0.6 (34) | 77.0 ± 13.1* (34) | 25.0 ± 0.3 (33) | 36.7 ± 0.7 (24) | 79.8 ± 21.0* (24) |
| Location | | | | | | | | | |
| Motor | 22.9 ± 0.4 (15) | 34.0 ± 0.8 (15) | 68.3 ± 18.5 (15) | 22.6 ± 0.4 (15) | 32.9 ± 0.8 (15) | 95.4 ± 23.6 (15) | 25.5 ± 0.4 (15) | 37.6 ± 1.1 (11) | 90.7 ± 27.1 (11) |
| Somatosensory | 22.5 ± 0.7 (7) | 33.5 ± 1.3 (7) | 66.1 ± 43.1 (7) | 22.4 ± 0.5 (7) | 32.8 ± 1.4 (7) | 98.5 ± 47.6 (7) | 24.8 ± 0.6 (7) | 38.7 ± 1.2 (3) | 198.2 ± 167.4 (3) |
| Distant | 22.3 ± 0.4 (29) | 32.6 ± 0.7 (29) | 64.9 ± 10.1 (29) | 22.1 ± 0.4 (30) | 32.3 ± 0.7 (30) | 97.0 ± 14.7 (30) | 24.6 ± 0.3 (27) | 36.6 ± 0.7 (20) | 113.6 ± 28.2 (20) |
| Total | 22.5 ± 0.3 (51) | 33.5 ± 0.5 (51) | 66.0 ± 9.6 (51) | 22.3 ± 0.2 (52) | 32.5 ± 0.5 (52) | 96.8 ± 12.3 (52) | 24.9 ± 0.2 (49) | 37.1 ± 0.6 (34) | 116.1 ± 25.2 (34) |

Values are means ± SE, nos. in parentheses are number of patients. SEPs, somatosensory evoked potentials. *Significantly different at $P < 0.05$.

## RESULTS

### *Cortical surface recordings*

Representative recordings using a 64-electrode array are shown in Fig. 1. Thirty-two locations (alternate rows of the grid) were recorded simultaneously, and all recordings were made within a period of 15 min. Isolatency lines at the peaks of the major potentials to be described aid in their identification in different columns. In this example the patient was operated under general anesthesia, and cortical stimulation was not carried out; identification of somatosensory cortex, motor cortex, and their associated sulci was made by SEP criteria described previously (Wood et al. 1988). In the case of patients operated under local anesthesia, cortical stimulation (e.g., Fig. 5) provided independent identification. From locations posterior to the central

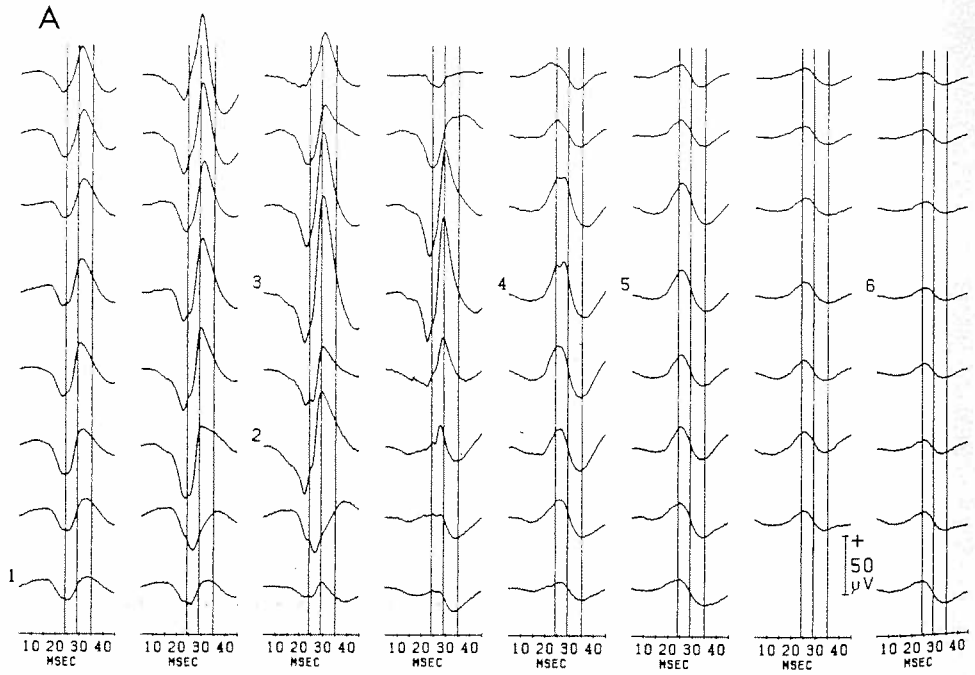


FIG. 3. SEP waveforms and topographic maps. *A: patient J23*; right frontal lobe astrocytoma abutting the hand area of motor cortex: general anesthesia. Array orientation as in Fig. 1. Isolatency lines are at the approximate peaks of P20–N20 (24 ms), a P25-like potential (29 ms) and N30–P30 (35 ms). *B*: maps at latencies of isolatency lines in *A*. *C*: waveforms at selected locations shown in *A* and *B*.



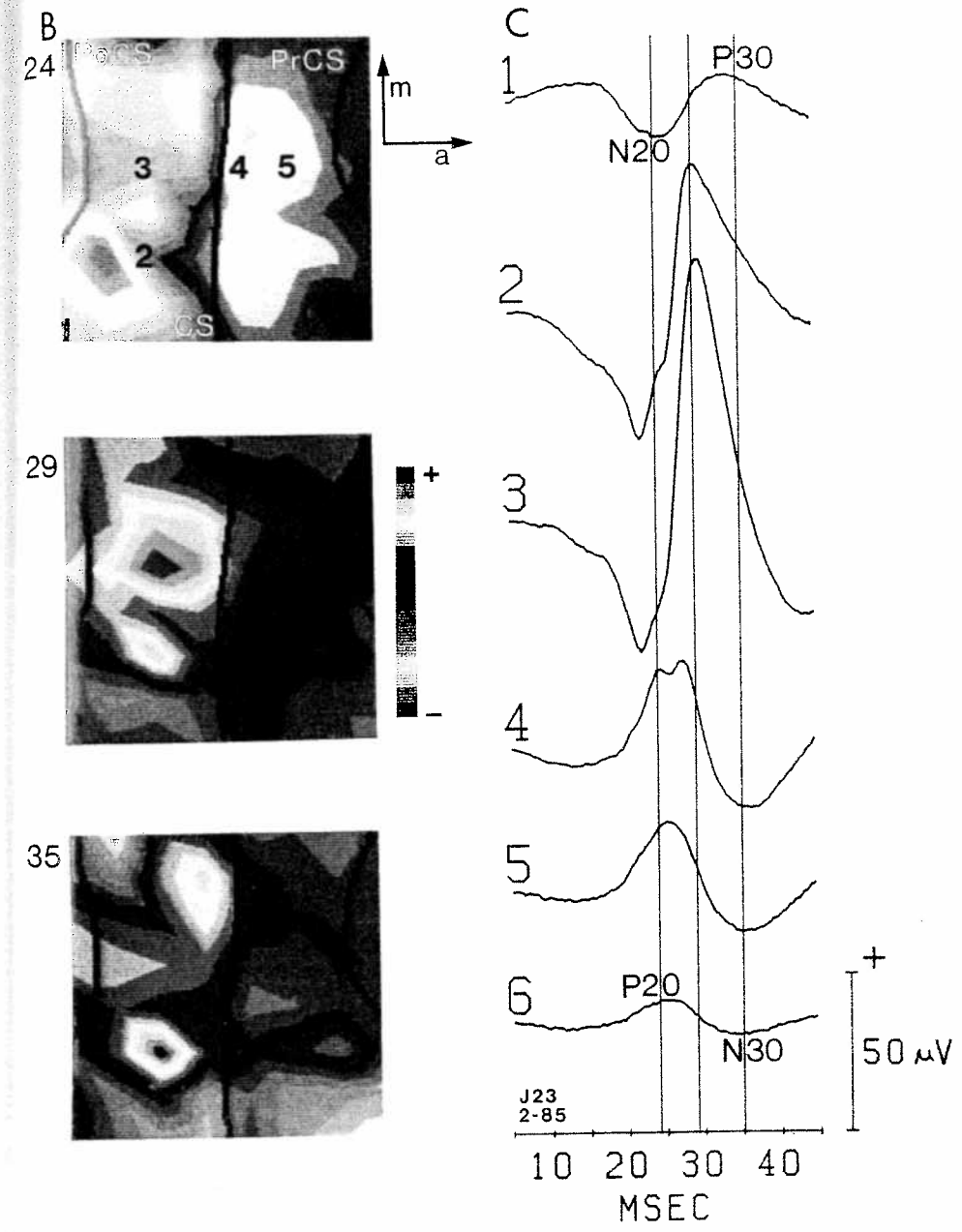


FIG. 3. (*continued*)

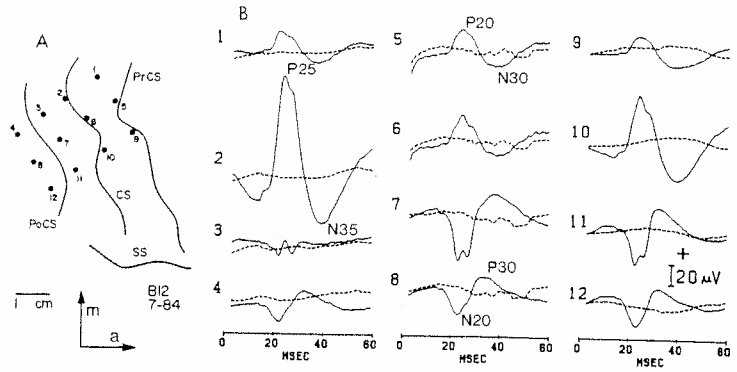


FIG. 4. SEP waveforms. *A: patient B12*; right frontal lobe astrocytoma distant from sensorimotor cortex; general anesthesia. *B*: SEPs to stimulation of the contralateral (——) and ipsilateral (– – –) median nerve.

sulcus (CS) over the lateral portion of the hand area of somatosensory cortex, negative-positive waveforms were recorded (e.g., *location 56*), and from precentral locations over motor cortex, approximately mirror-image waveforms were recorded (e.g., *location 36*). These postcentral and precentral potentials will be referred to as N20–P30 and P20–N30, respectively, corresponding to their polarity and average peak latency across patients. They were recorded in all patients in whom the hand representation area was exposed, with the exception of three patients with tumors involving the hand area in whom no SEPs could be recorded (Wood et al. 1988). The between-average variability of these potentials was small (see Fig. 2*C* of the following paper). In addition, a slightly later sequence of potentials, P25–N35, was recorded from the medial portion of the hand area of somatosensory cortex (e.g., Fig. 1, *location 7*). P25–N35 was recorded as a distinct entity in 30% of the cases, but in 35% of the cases P25 was seen only as an inflection on the rising phase of P30 and was not followed by a distinct N35. Thus P25–N35 appeared to be less robust than P20–N30 and N20–P30, although some failures to record it with large amplitude may have resulted from incomplete exposure of the medial portion of the hand area or to nonoptimal electrode placements. At the locations where they were largest, the identification and measurement of all these potentials presented no problems, but at intermediate locations transitional waveforms were seen (e.g., Fig. 1*B*, *location 38*; Fig. 2*A*, just posterior to *location 6*) that could not necessarily be categorized in the same manner.

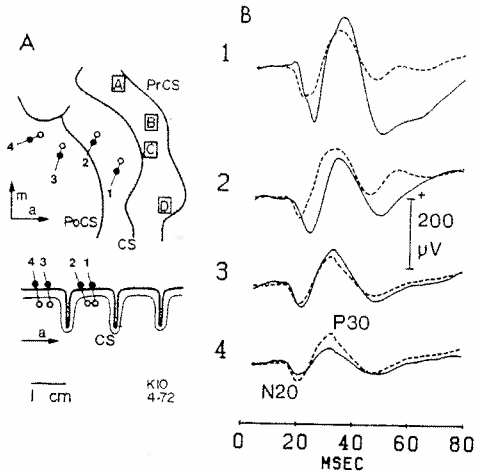


FIG. 5. Transcortical recordings from postcentral cortex. *A: patient K10*; right parietal lobe glioma in the face area of somatosensory cortex; local anesthesia. Cortical stimulation: A, arm abduction; B, forearm flexion; C, hand flexion; D, eyelid and neck movement. In this and Fig. 6, all motor responses refer to contralateral side of body except for perioral responses, and the *bottom drawing* is a schematic quasisagittal view of locations of surface (●) and estimated locations of deep (○) electrodes of the transcortical pairs. *B*: SEPs from surface (——) and deep (– – –) electrodes.

Table 1 summarizes peak latencies and amplitudes of these potentials. The results were stratified in three ways: *1*) by comparing SEPs obtained under local or general anesthesia, *2*) by the location of brain pathology (abutting or invading motor cortex, abutting or invading somatosensory cortex, or distant from sensorimotor cortex), and *3*) by the type of pathology (primary epileptogenic region, tumor, or miscellaneous other). Analysis of variance showed that amplitudes were significantly decreased by general anesthesia compared with local anesthesia (P20–N30: $F = 6.6$, $P < 0.02$; N20–P30: $F = 4.9$, $P < 0.04$; P25–N35: $F = 5.0$, $P < 0.04$). The location of pathology (Table 1) and type of pathology (not shown in Table 1) did not have a systematic effect on SEPs, suggesting that these recordings were not compromised by the patients' pathology.

Waveform plots (e.g., Fig. 1*B*) display variations in voltage as a function of time and emphasize the temporal dimension of the data. Topographic maps, such as those in Fig. 1*C*, emphasize the spatial dimension of the data by displaying the distribution of voltage at a number of latencies, in this case at 1-ms intervals from 20–39 ms poststimulus. The map at 22 ms illustrates the spatial SEP distribution at the peak of N20–P20, indicated by the first isolatency line in Fig. 1*B*. This distribution has two extrema, negative postcentrally and positive precentrally. The distribution at 26 ms (the peak of P25; the 2nd isolatency line) had a positive maximum over somatosensory cortex: this maximum was medial to the N20 minimum and extended across the CS into motor cortex. The distribution at 31 ms (the peak of P30–N30; the 3rd isolatency line) was similar in shape to the one at 22 ms but was opposite in polarity. The distribution at 39 ms (the peak of N35) was similar in shape to the one at 26 ms but was opposite in polarity. At latencies between the isolatency lines, the distributions had shapes and polarities intermediate to those described.

Figure 2 shows another example of SEPs in relation to the anatomy of sensorimotor cortex. All 64 waveforms are shown in Fig. 2*A*, and selected waveforms are shown at higher resolution in Fig. 2*C*. From precentral (e.g., *location 6*) and postcentral (e.g., *location 1*) sites, approximate mirror-image waveforms were recorded, corresponding to P20–N30 and N20–P30. The distribution at the approximate peak of P20–N20 (Fig. 2*B* at 22 ms) consists of a postcentral minimum and a precentral maximum, with the zero-potential line at the CS. From *location 4* on the medial portion of the postcentral hand area P25 was recorded, corresponding to the maximum in the *top left* portion of the map at 25 ms. Similar results are shown in Fig. 3. At sites relatively distant from the CS, precentral (*location 6*) and postcentral (*location 1*) mirror-image waveforms were recorded (Fig. 3, *A* and *C*). P20–N20 is seen in the distribution at 24 ms as a precentral maximum and a postcentral minimum. Nearer the CS (*locations 2–5*) the waveforms were more complex (see below).

To summarize, these SEPs have different spatial characteristics. P20–N30 was largest over the hand area of motor cortex and often extended anterior to motor cortex. N20–P30 was largest over the lateral portion of the hand area of somatosensory cortex and often extended posteriorly over the supramarginal gyrus. These precentral and postcentral potentials were approximate mirror images of one another at locations relatively distant from the CS. P25–N35 was largest in the anteromedial portion of the hand area of somatosensory cortex near the CS and often extended anteriorly onto motor cortex.

In addition to the SEPs just described, additional positive SEPs were sometimes recorded that appeared to be discriminable from P20, P25, and P30. Like P25, this activity was largest over somatosensory cortex near the CS but was also seen at precentral locations near the CS (Fig. 2). At 29 ms, a potential different from P25 (note the presence of both potentials at *location 5*) was recorded that had a more lateral maximum than P25. The maxima at 25 and 29 ms appeared to be separate and fixed; note the presence of both maxima at 25 ms, interrupted by a low-voltage region. The maps between 25 and 29 ms (not shown) showed a gradual decrease of voltage in the medial P25 distribution and a gradual increase in the lateral P25-like distribution. At 36 ms an even more lateral positivity was seen with a maximum near *location 3*. Again the distributions between 27 and 36 ms (not shown) suggested the presence of two spatially separate regions of positivity.

In Fig. 3 the peak at ~29 ms, largest at *location 3* and corresponding to the postcentral maximum in the distribution at 29 ms, probably corresponds to the 29-ms potential of Fig. 2. In addition, positive potentials were seen at ~25 and 27 ms (*location 4*), but which of these corresponds to P25 is unclear. A later positivity was seen at ~35 ms as a prolongation of positivity after the peak at 29 ms (*location 2*) and as a maximum in the lateral portion of the



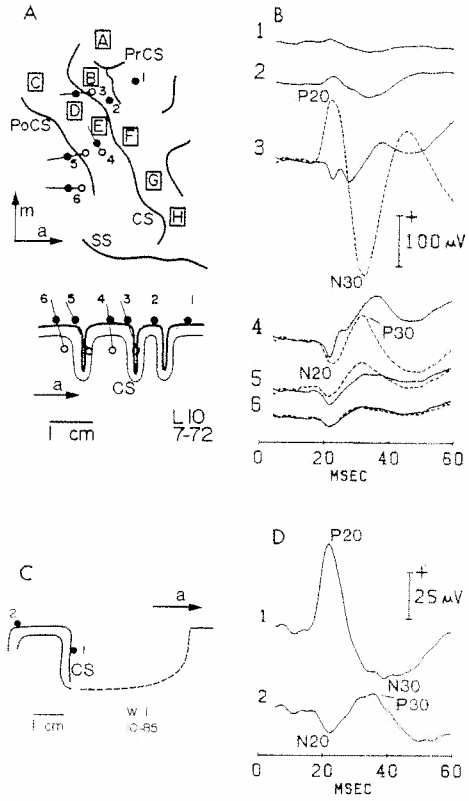


FIG. 6. Surface and transcortical recordings. *A: patient L10*; right frontal lobe epileptogenic region distant from sensorimotor cortex; local anesthesia. Cortical stimulation: A, shoulder movement; B, arm movement; C, hand movement; D, 3rd digit movement; E, thumb movement; F, head and back movement; G, mouth movement; H, jaw and throat movement. (In this patient, only motor responses were obtained to stimulation of both motor and somatosensory cortex as determined by SEP recording.) *B*: SEPs from surface (——) and deep (– – –) electrodes. *C. patient W1*; Rasmussen's Syndrome involving the hand area of right motor cortex; general anesthesia. Sagittal view of electrodes placed on the exposed anterior wall (1) and crown (2) of somatosensory cortex after removal (– – –) of the hand area of motor and premotor cortex. *D*: SEPs recorded from locations in *C*.

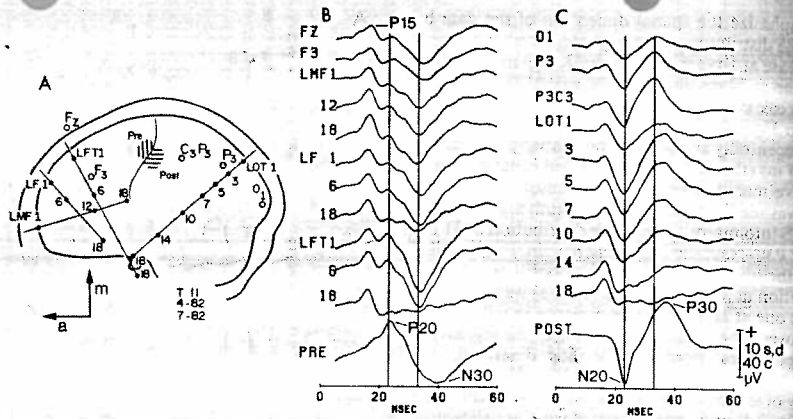


FIG. 7. Depth-probe, cortical-surface, and scalp recordings. *A: patient T11*; left temporal lobe epileptogenic region distant from sensorimotor cortex. In this and the next figure, depth-probe locations were determined by lateral X-ray; other recording locations were projected onto the X-ray view. Left occipitotemporal (LOT), frontotemporal (LFT), frontal (LF), and mesiofrontal (LMF) probes were, respectively, 31, 29, 22, and 21 mm from the midline. Lateral scalp electrodes were ~7 cm from the midline. Surface of sensorimotor cortex was ~5.5 cm from the midline; precentral (Pre) and postcentral (Post) recordings were made approximately from the hatched regions shown. *B*: precentral recordings; Pre is the mean of the SEPs recorded from 9 motor cortex locations. *C*: postcentral recordings; Post is the mean of the SEPs recorded from 9 somatosensory cortex locations. Scalp and depth-probe recordings were made while the patient was awake and unsedated, 3 mos before cortical surface recordings obtained under local anesthesia. Isolatency lines are at the approximate peaks of P20–N20 (23 ms) and N30–P30 (33 ms) recorded preoperatively. Voltage calibration: s, scalp recordings; d, depth recordings; c, cortical surface recordings.

map at 35 ms. Both maxima are seen in the distribution at 29 ms. The first of these P25-like potentials (e.g., Fig. 2, *location 5*, and distribution at 29 ms) was seen in a number of recordings. The second (e.g., Fig. 2, *location 3*, and distribution at 36 ms) was seen less frequently. Just as P25 was often followed by N35, the P25-like potentials were sometimes followed by a possibly corresponding negativity in the 40 to 50-ms latency range (Fig. 3, *location 3*). To summarize, in some recordings later P25-like potentials were seen in the central and lateral portion of the hand area of somatosensory cortex near the CS.

In 13 patients recordings were made to stimulation of the ipsilateral as well as contralateral median nerves. Figure 4 compares SEPs evoked by ipsilateral and contralateral stimulation. The contralateral SEPs were similar to those already described. By contrast, in this and other recordings, no detectable activity in the 20 to 40-ms latency range was evoked by ipsilateral stimulation.

*Transcortical recordings*

In the first five patients in whom cortical surface recordings were obtained, transcortical recordings from somatosensory cortex were also obtained because it had been suggested that surface recordings alone could not provide definite localization of the sensorimotor hand area (Kelly et al. 1965). However, results from these cases indicated that surface recordings were sufficient for localization, and it was felt that continued transcortical recording was not clinically justified. The locations of the surface electrodes of the transcortical pairs and the trajectories of the deep electrodes were determined from photographs made in surgery. However, in the absence of histological verification, the exact locations of the deep electrodes in relation to cortex in the walls of the CS and PoCS are unknown.

The transcortical recordings of Fig. 5 yielded N20–P30 both at the surface and from corresponding sites in white matter of somatosensory cortex (*locations 1* and *2*) and from surface and deep sites in the supramarginal gyrus (*locations 3* and *4*). Similarly, in the transcortical recordings of Fig. 6*B*, N20–P30 was recorded from surface and deep electrodes in the postcentral and supramarginal gyri (*locations 4–6*). By contrast, *electrode 3* deep recorded a P20–N30 that was much larger than the largest P20–N30 recorded from the surface of motor cortex (*location 2*). *Electrode 3* deep was probably near the surface of the posterior wall of the CS (Fig. 6*A*), thus *electrodes 3* deep and *4* deep demonstrated a polarity inversion across the posterior wall of the CS. Similar results were obtained in two other cases (e.g., Fig. 8, *location 4* of the following paper). Transcortical recordings were not informative in the fifth patient, in whom the hand area was not well exposed.

Another recording across the posterior wall of the CS is shown in Fig. 6*D*. An electrode (*location 1*) was placed on the exposed surface of the posterior wall of the CS following removal of motor cortex to the fundus of the CS (Fig. 6*C*). A large P20–N30 was recorded from this location, whereas a smaller N20–P30 was recorded from the crown of somatosensory cortex (*location 2*). Note the similarity in waveform of these potentials to those recorded, respectively, from *locations 3* deep and *4* surface of Fig. 6*B*.



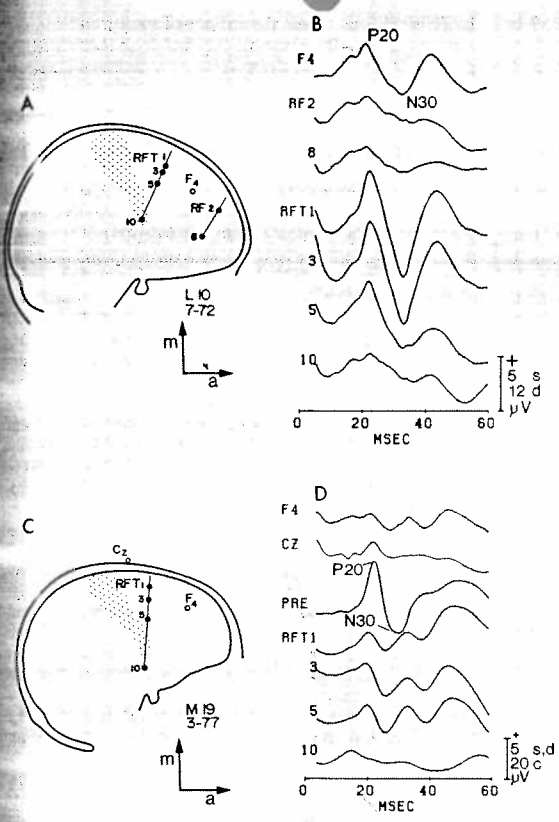


FIG. 8. Depth-probe, cortical-surface, and scalp recordings. *A: patient L10*; right frontal lobe epileptogenic region distant from sensorimotor cortex. The RFT and RF probes were, respectively, 25 and 27 mm from the midline. Stippled region indicates range of trajectories of the CS (Talairach and Szikla 1967); *locations 1–5* on the RFT probe were ~4 cm anterior to the CS in the hand area. *B*: scalp and depth-probe recordings were made while the patient was awake and unsedated, the day before the intraoperative recordings shown in Fig. 6*B*. *C: patient M19*; right frontal lobe epileptogenic region distant from sensorimotor cortex. The RFT probe was 31 mm from the midline, *locations 1–5* were ~3 cm anterior to the CS. *D*: scalp and depth-probe recordings were made while the patient was awake and unsedated, 3 mos before the intraoperative recordings obtained under local anesthesia; Pre is the mean of the cortical surface SEPs recorded from 7 precentral locations.

To summarize, these recordings suggested a polarity inversion from P20–N30 to N20–P30 across the posterior wall of the CS, but did not show polarity inversion of either N20 or P30 across the crowns of the postcentral and supramarginal gyri.

*Depth-probe recordings*

Intracranial depth probes, although not placed in sensorimotor cortex, allowed recordings from many regions of the brain and thus provided additional characterization of the intracerebral distribution of SEPs generated in sensorimotor cortex. They also allowed the opportunity to record potentials possibly generated in other cortical regions.

Figure 7 shows four depth probes implanted in the left hemisphere to localize a possible frontal or temporal epileptogenic focus. Several days after implantation, while the patient was awake and unsedated, SEPs were recorded from many depth-probe and scalp locations; representative examples are shown in Fig. 7, *B* and *C*. P15, seen at approximately the same amplitude at all depth-probe and scalp locations, is of subcortical origin (Allison et al. 1980; Chiappa 1983; Desmedt and Cheron 1981); because of the use of a cerebral reference electrode, it was less evident in cortical-surface recordings (*bottom traces*), obtained 3 mos later during removal of the left anterior temporal lobe. The waveforms labeled Pre and Post are the mean P20–N30 and N20–P30 waveforms recorded, respectively, from all precentral and postcentral cortical surface locations; this procedure avoids bias in selecting a particular cortical surface waveform for comparison with waveforms recorded at a distance from sensorimotor cortex. The peak latencies of N30 and P30 were a few milliseconds later in the intraoperative recordings compared with the scalp and depth-probe recordings. Such latency changes were often observed (also see Fig. 8) and were probably because of intraoperative sedative, anesthetic, and brain cooling effects (Broughton 1969). P20–N30 was recorded from all frontal scalp and depth-probe locations; it was similar to those recorded from the cortical surface but was smaller in amplitude (note different voltage calibrations). Similarly, N20–P30, similar in waveform but smaller than the N20–P30 recorded from the cortical surface, was recorded

from all frontal and occipital depth-probe and scalp locations.

Figure 8 shows SEPs recorded from frontal depth-probe and scalp locations. In these cases recordings were obtained from closely spaced electrodes near frontal cortex (*locations 1, 3,* and *5*). P20–N30 recorded from all frontal depth-probe and scalp locations (Fig. 8*B*) was similar in waveform to, but much smaller than, P20–N30 later recorded intraoperatively from precentral (*2* and *3* deep) locations (Fig. 6*B*). Similarly, in another patient (Fig. 8, *C* and *D*), P20–N30 recorded from all depth-probe and scalp locations was similar in waveform to, but much smaller than, the mean precentral (Pre) P20–N30 later recorded intraoperatively from the cortical surface. In both depth-probe recordings of Fig. 8, the largest P20–N30 was recorded from *electrode 3* (located ~1 cm below the cortical surface), with slightly smaller amplitude above and below it.

The depth-probe and scalp recordings of Figs. 7 and 8 are representative of those obtained in 12 patients. The mean peak-to-peak amplitudes of P20–N30 measured from the precentral F and FT probes, and N20–P30 measured from the postcentral OT probes, were 4.7, 10.4, and 7.5 $\mu$V, respectively. There was no evidence in any recording of polarity inversion of P20–N30 and N20–P30 from locations above the cortical surface to locations below it. P20–N30 was largest below the cortical surface and smaller superficially and deeper. In all cases SEPs recorded from depth probes were similar in waveform to but smaller than those recorded from sensorimotor cortex; thus there was no evidence in these recordings of activity generated outside sensorimotor cortex.

## DISCUSSION

### *Potentials attributed to area 3b*

A consistent feature of these recordings is the presence of P20–N30 and N20–P30, which are approximate mirror images of one another in recordings from motor and somatosensory cortex, respectively (Figs. 1–6; also see Allison et al. 1980, 1982; Broughton et al. 1969, 1981; Lueders et al. 1983; Wood et al. 1985, 1988). Two alternative hypotheses to explain this result have been proposed. The first asserts that these potentials are generated in *area 3b* of somatosensory cortex (Allison et al. 1980; Broughton 1969), which in humans and Old World monkeys is located in the posterior wall of the CS (Bailey and von Bonin 1951; Braak 1980; Powell and Mountcastle 1959a; Vogt 1928). In cortical-surface recordings, an abrupt change in polarity across a sulcus would be a natural consequence of potentials generated within a wall of the sulcus. Such polarity inversions were a major impetus for the initial proposal that P20–N30 and N20–P30 are generated in *area 3b* (Broughton 1969). The second hypothesis asserts that P20–N30 and N20–P30 are independently generated in the crowns of motor and somatosensory cortex, respectively (Desmedt and Cheron 1981; Papakostopoulos and Crow 1984). Cortical-surface recordings alone do not allow a clear choice between the two hypotheses. However, they make different predictions about the potential distribution in and beneath cortex. The second hypothesis predicts polarity inversions across surface of motor and somatosensory cortex. By contrast, the first hypothesis predicts polarity inversion and sharp voltage gradients of P20–N30 and N20–P30 across *area 3b*, but not across cortex in the crowns of motor and somatosensory cortex. The pertinent results, which strongly favor the hypothesis that these potentials are generated in *area 3b*, may be summarized as follows:

1) There is no evidence of generation of P20–N30 and N20–P30 in precentral or postcentral surface cortex: a) Precentral scalp, cortical-surface, and depth-probe recordings showed similar P20–N30 waveforms (Figs. 7 and 8), indicating that P20–N30 is not generated in surface cortex of the frontal lobe. b) Postcentral scalp, transcortical, and depth-probe recordings showed similar N20–P30 waveforms (Figs. 5*B*, 6*B*, and 7*C*), indicating that N20–P30 is not generated in surface cortex of the parietal lobe.

*2*) The cortical-surface and intracerebral distribution of potentials is consistent with an origin within a wall of the CS: a) P20–N30 and N20–P30 were largest at locations within the CS, and the decrease in voltage at more distant sites was similar to that predicted by generators located in somatosensory cortex (Fig. 10). b) In depth-probe recordings from the frontal lobe, P20–N30 was largest 1–2 cm below the cortical surface (Fig. 8). The human CS is ~1.8 cm deep (mean of 6 hemispheres), and the center of the CS is thus ~1 cm below the surface. The potential field produced by a source within the CS would exhibit a maximum slightly below the surface of frontal cortex, in agreement with the empirical results (Fig. 8) but inconsistent with an origin in surface cortex of the frontal lobe. c) The results just described are consistent with a generator located in either wall of the CS. However, P20–N30 and N20–P30 can be recorded after removal of the hand area of motor cortex (Fig. 6*D*), indicating that a generator in the anterior wall of the CS can be ruled out.

*3*) Polarity inversion from P20–N30 to N20–P30 across the posterior wall of the CS (e.g., Fig. 6*B*) strongly suggests that *area 3b* generates these potentials. The uncertainty in these recordings about the exact locations of the deep electrodes in relation to cortex in the walls of the CS does not apply to the recording of Fig. 6*D*, which was made from an electrode placed directly on the posterior wall of the CS after resection of motor cortex. The large P20–N30 recorded from this location was similar to that recorded from *electrode 3* deep of Fig. 6*B*, and both were the largest potentials recorded from any surface or deep site in these cases.

SEP and multiunit recordings from Old World monkeys demonstrate that potentials corresponding to the human P20–N30 and N20–P30 are generated in *area 3b* (Arezzo et al. 1979, 1981). Anterior to the CS, P10–N20 similar in waveform to the human P20–N30 (but shorter in latency because of the shorter conduction pathway) were recorded. P10–N20 was recorded with similar latency and waveform at all precentral surface and depth sites, in agreement with our human recordings. Posterior to the CS, N10–P20 was recorded, corresponding to the human N20–P30. P10–N20 showed polarity inversion across *area 3b* but not across *areas 1* and *2*, in agreement with the human results. P10 was associated with strong unit discharges in *area 3b* but not in *area 4*. Lesions of motor cortex have little effect on P10–N20 and N10–P20, whereas lesions of somatosensory cortex abolish them (Allison et al. 1986). Thus these monkey recordings support the conclusion that the human P20–N30 and N20–P30 are generated only in *area 3b*.

### *Potentials attributed to area 1*

P25–N35 was largest in the anteromedial portion of the hand area of somatosensory cortex (Figs. 1–3; also see Wood et al. 1988). It did not invert in polarity across the CS and was recorded at smaller amplitude from motor cortex near the CS and from the posterior crown of somatosensory cortex. This potential distribution suggests a generator in *area 1*, which in humans and Old World monkeys is located primarily in the anterior crown of the postcentral gyrus (Powell and Mountcastle 1959a; Vogt 1928). Our transcortical recordings were made before the spatial differentiation of P25–N35 and N20–P30 was appreciated, and, as it happened, we did not obtain transcortical recordings of P25–N35. However, transcortical recordings in 41 patients (Goldring et al. 1970; Kelly et al. 1965; Stohr and Goldring 1969) from postcentral sites near the CS showed a surface positivity in the 23 to 27-ms latency range followed by a negativity in the 35 to 40-ms latency range, with polarity inversion in white matter. These potentials correspond to P25–N35 as described here and thus confirm their primary origin in *area 1*. In monkeys P12–N25, corresponding to the human P25–N35, was recorded from *area 1* (Arezzo et al. 1979, 1981; also see Gardner et al. 1984; Kulics and Cauller 1986). P12–N25 inverted in polarity from surface to white matter, in agreement with human transcortical recordings (Goldring et al. 1970; Stohr and Goldring 1969).

The later P25-like potentials had spatial distributions similar to that of P25 except that they were largest over the central and lateral portion of the hand area of somatosensory cortex. We surmise that these potentials are also generated in *area 1*. Their maxima appear to be spatially fixed (Figs. 2 and 3), suggesting a medial (P25) to lateral (later P25-like potentials) sequence of activation of separate regions in *area 1*. Perhaps each locus corresponds to activation of the representation of the three digits (thumb and first two fingers) innervated by the median nerve. A more likely possibility is that spatially discrete regions of *area 1* respond to a peripheral stimulus. Two and sometimes three separate patches of 2-deoxyglucose labeling are evident in *area 1* of monkey somatosensory cortex following flutter stimulation of a single finger (Juliano and Whitsel 1985). There is also evidence of serial activation of these patches by corticocortical pathways within *area 1* (Juliano et al. 1987), although the patches appear to be reciprocally connected and thus offer no clue regarding a possible spatiotemporal sequence of activity. However, the monkey and human results as a whole suggest a sequential mediolateral activation of separate patches of *area 1* to finger or median nerve stimulation. There is no evidence in the human recordings of a similar mediolateral activation of *area 3b*.

### *Potentials possibly generated in areas 4, 3a, and 2*

Somatosensory afferent projections to *area 4* of motor cortex are sparse compared with those to *area 3b* (Jones and Powell 1970), but nevertheless short-latency unit discharges and SEPs have been recorded in *area 4* of cats and monkeys by many investigators (e.g., Jones 1983; Wiesendanger 1973). Our recordings do not provide strong evidence for or against the generation of SEPs in human *area 4* because we did not attempt to make transcortical recordings from this area. Kelly et al. (1965) initially reported that transcortical SEPs indicative of local generation could not be recorded from motor cortex, but later this group (Goldring et al. 1970; Stohr and Goldring 1969) found that potentials usually smaller and slightly later than those recorded from somatosensory cortex (corresponding to P25–N35 as noted above) could sometimes be recorded from the crown of motor cortex and appeared to be generated therein. In awake monkeys a later P12-like potential (P13) was recorded from motor cortex. These results suggest that SEPs generated in motor cortex could contribute to P25–N35 in some cases. On the other hand, surgical removal of the hand area of somatosensory cortex abolishes all median nerve SEPs in humans (Allison et al. 1984; Stohr and Goldring 1969; Wood et al. 1986) and monkeys (Allison et al. 1986), whereas removal of the hand area of motor cortex in monkeys has little effect (Allison et al. 1986). Motor cortex makes no detectable contribution to SEPs elicited by airpuff stimulation of the hand in awake monkeys (Gardner et al. 1984). These results suggest that motor cortex makes little or no contribution to SEPs recorded from the surface of sensorimotor cortex.

It has been suggested that *area 3a* contributes to short-latency SEPs (Gandevia et al. 1984; Jones and Power 1984) and magnetic fields (Kaukoranta et al. 1986) evoked by median nerve stimulation and recorded extracranially. A tactile interference technique (Jones and Power 1984) performed in eight patients of this series suggests that an early fraction of P20–N20 may be generated in *area 3a*, although a recent study (Halonen et al. 1988) suggests that the contribution of muscle afferents to median nerve SEPs recorded from the scalp is small.

In humans and Old World monkeys, *area 2* occupies the posterior one-half of the crown of somatosensory cortex and the anterior wall of the PoCS in the hand representation (Powell and Mountcastle 1959a; Vogt 1928). P25–N35 was largest (Figs. 1–4) in the anterior one-half of the crown of somatosensory cortex, and transcortical recordings from *area 2* (e.g., Fig. 5, *location 2*) did not show evidence of locally generated activity. The transcortical recordings of Kelly et al. (1965) and Stohr and Goldring (1969), which showed polarity inversion from surface to white matter, and for which recording locations are shown, appear to have been made from *area 1*, although one such recording (Stohr and Goldring 1969, Fig. 4, *location D*) may have been from *area 2*. Thus there is little evidence that *area 2* contributes to SEPs recorded from the cortical surface.

The stimulating and recording conditions of the present study may have biased the recordings toward the more cutaneous regions (*areas 3b* and *1*) of sensorimotor cortex:

*1*) The human median nerve at the wrist is composed mainly of cutaneous fascicles (Schady et al. 1983; Sunderland and Bedbrook 1949), and stimulation of motor branches in the arm evokes only small, ill-defined poten-

tials on scalp (Halonen et al. 1988). *Area 4* receives input fr cutaneous and deep receptors, but most *area 4* neurons are preferentially sensitive to movement of joints (Lemon and van der Burg 1979). *Area 2* receives input primarily from joint receptors, and *area 3a* primarily receives the projection of group I muscle afferents (Jones 1983; Powell and Mountcastle 1959b). These considerations suggest that stimulation of the median nerve at the wrist may produce relatively little activation of neurons in *areas 4, 3a,* and *2*.

*2*) Although some neurons in *area 2* respond to synchronous inputs of the sort provided by whole nerve shocks (e.g., Arezzo et al. 1981; Kaas et al. 1981; Powell and Mountcastle 1959b), others are preferentially responsive to complex spatiotemporal patterns of activity (e.g., Iwamura et al. 1980).

*3*) It has been reported in monkeys that neurons in *area 4* (Wiesendanger 1973) and *area 2* (Powell and Mountcastle 1959b) are sensitive to anesthetic effects. The patients of this study who were operated under local anesthesia received analgesics (usually fentanyl) and neuroleptics (usually droperidol), and those operated under general anesthesia also received a short-acting barbiturate (pentothol) during induction, followed by nitrous oxide and a halogenated anesthetic (usually isoflurane) in oxygen. It is possible that these agents selectively affected potentials in *areas 4* and *2* more than potentials in *areas 3b* and *1*.

*Ipsilateral potentials*

Stimulation of the ipsilateral median nerve produced no detectable activity in our and other human cortical surface recordings (Fig. 4; also see Goldring et al. 1970; Lueders et al. 1983; Wood et al. 1988), consistent with the common observation that neurons in the hand area of monkey somatosensory cortex respond only to contralateral stimulation (Kaas et al. 1981; Powell and Mountcastle 1959b; Werner and Whitsel 1973). Very small (~2 $\mu$V) ipsilateral potentials have been recorded from somatosensory cortex in exceptional cases (Lueders et al. 1986); whether this activity is locally generated has not been established. In deeper layers of cat somatosensory cortex, some neurons (*m* neurons) respond to ipsilateral stimulation (Towe 1966), but their activation contributes negligibly to the SEPs corresponding to the human P20–N30 and P25–N35. If *m* neurons are present in human somatosensory cortex, their activation apparently does not generate short-latency potentials consistently recordable at the cortical surface. However, at longer latencies ipsilateral potentials of apparently local origin can be recorded (Allison et al. 1989).

*A model of electrogenesis in areas 3b and 1*

The results of this study suggest that *area 3b* generates a surface positive-negative sequence (P20–N30) and that *area 1* generates a similar sequence (P25–N35) a few millisecond later. Thus activation of human somatosensory cortex by a discrete peripheral stimulus appears to generate the same surface positive-negative sequence of potentials recorded from somatosensory cortex of monkeys (Allison et al. 1986; Arezzo et al. 1979, 1981; Gardner et al. 1984; Wood and Allison 1981; Zimmerman 1968), cats (Allison et al. 1966; Mitzdorf 1985; Perl and Whitlock 1955; Schlag 1973; Towe 1966) and other mammals (Allison et al. 1980; Woolsey and Fairman 1946). These positive-negative sequences are often called the primary evoked response (Towe 1966) and have been recorded from visual, auditory, and somatosensory cortex (Mitzdorf 1985; Schlag 1973; Towe 1966). The primary positivity is thought to reflect the initial depolarization of pyramidal cell bodies and proximal apical dendrites, whereas the primary negativity is thought to reflect the later depolarization of the distal portion of apical dendrites (Creutzfeldt and Houchin 1974; Landau 1967; Schlag 1973; Werner and Whitsel 1973; Wood and Allison 1981; for somewhat different views see Dykes 1978; Towe 1966).

The hypothesis that the temporal and spatial patterns of cortical surface SEPs are generated by *areas 3b* and *1* was tested using a model of electrogenesis based on electric field theory (Fig. 9). Cortical generators corresponding to *areas 3b* and *1* were represented in the model by two dipole sources with fixed locations and orientations. Single dipole sources were employed instead of sheets of dipoles because the surface fields generated by a dipole sheet can, to a first approximation, be accounted for by the field of a single dipole located at the centroid of the sheet and oriented perpendicular to it (e.g., Darcey 1979).

The locations and orientations of the *area 3b* and *area 1* generators were specified as follows. Based on human anatomic measurements (see above), the dipole representing the centroid of *area 3b* was placed 9 mm below the cortical surface. In the anterior-posterior dimension it was placed 1 mm posterior to the CS, representing the upper and middle cortical layers where current sinks of the primary potentials are seen in animal recordings (Dykes 1978; Mitzdorf 1985; Perl and Whitlock 1955; Towe 1966; Werner and Whitsel 1973). The CS was assumed to be a plane oriented perpendicular to the cortical surface (Fig. 9*B*), and the *area 3b* dipole was therefore oriented tangential to the cortical surface. The postcentral gyrus is ~16 mm wide (mean of 46 cases) in the hand representation, and *area 1* occupies its anterior half (Powell and Mountcastle 1959a; Vogt 1928); the dipole representing the centroid of *area 1* was thus placed 4 mm posterior to the CS and 1 mm below the cortical surface for the reason noted above. It was tilted 10° toward the CS because *area 1* lies primarily in surface cortex and partly in the upper portion of the posterior wall of the CS (Powell and Mountcastle 1959a; Vogt 1928). The average distance between the P25 and N20 extrema is 9.9 mm (Wood et al. 1988); the *area 1* dipole was therefore placed 1 cm medial to the *area 3b* dipole. This apparent mediolateral displacement of the hand representations of *area 3b* and *area 1* is not evident in somatotopic maps of somatosensory cortex in anesthetized monkeys (e.g., Kaas et al. 1981) but is consistent with other studies. Monkey ventrobasal thalamic neurons responding to finger stimulation project to a region of *area 1* medial to the projection to *area 3b* (Jones et al. 1982). Similarly, the center of 2-deoxyglucose labeling of cynomolgus monkey *area 1* to finger stimulation is ~3–4 mm medial to (although it overlaps with) the center of labeling in *area 3b* (Juliano and Whitsel 1985). The mediolateral extent of somatosensory cortex is ~3.5 cm (mean of 8 hemispheres) in cynomolgus monkeys and ~10 cm (mean of 6 hemispheres) in humans. Assuming a similar projection of the body surface onto somato-

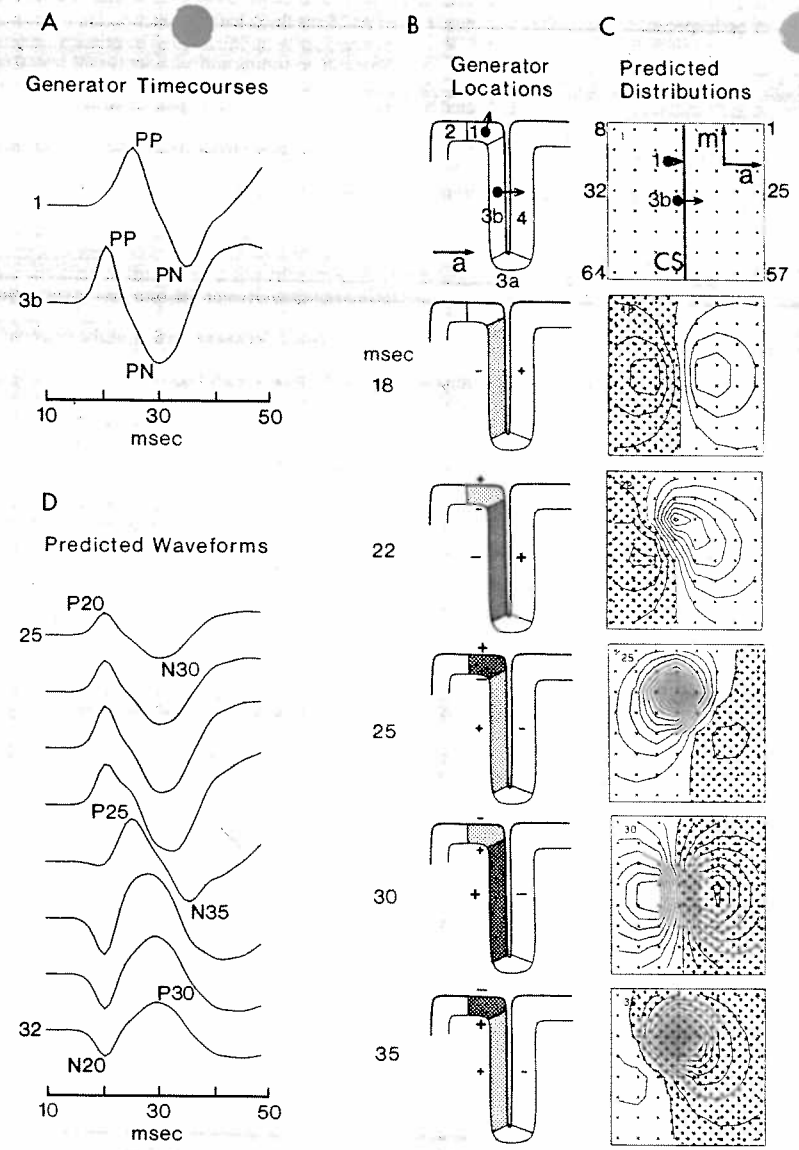


FIG. 9. Postulated electrogenesis of short-latency SEPs. *A*: *areas 3b* and *1* are hypothesized to generate the surface primary positive (PP) and primary negative (PN) potentials with the timecourses shown. *B*: schematic sagittal view of the right hemisphere hand representation area of sensorimotor cortex. *Top drawing*: location and orientation of the *area 3b* and *area 1* generators. *Bottom drawings*: degree of activation of an area at selected latencies is indicated by the density of stippling. *C*: schematic top view of the right hemisphere hand representation area. *Top drawing*: location and orientation of the *area 3b* and *area 1* generators in relation to the 64 locations at which voltages were calculated. *Bottom drawings*: isovoltage topographic maps at the latencies indicated in *B*. Clear areas indicate positive voltage, stippled areas negative voltage. *D*: calculated waveforms at *locations 25–32* shown in *C*.

sensory cortex of both species, the estimated distance between the centers of projections to *areas 1* and *3b* in humans would be ~9.7 mm, similar to the average distance of 9.9 mm between the P25 and N20 extrema. The locations of the *area 3b* and *area 1* dipoles are indicated by filled circles in Fig. 9, *B* (sagittal view) and *C* (surface view). Dipole orientations are illustrated by arrows, which, by convention, point toward the positive sides of the dipole fields. The orientations shown correspond to the primary positivities of *areas 3b* and *1*; corresponding dipole orientations for the primary negativities are 180° from those shown.

The timecourse of activation of these generators (Fig. 9*A*, *top*) simulated primary evoked responses recorded in animals (cited above). The dipole moments (amplitudes) of the two generators were adjusted to produce approximately equal amplitudes at the cortical surface. The *area 3b* and *area 1* timecourses were given absolute latencies comparable with the P20–N30 and P25–N35 latencies respectively. In other words, the *area 1* generator timecourse was delayed 5 ms compared with the *area 3b* timecourse. In monkeys the peak latency of the *area 1* primary response is also a few milliseconds later than the *area 3b* response (Allison et al. 1986; Arezzo et al. 1981; Zimmerman 1968), probably because thalamic afferents to *area 3b* are a dense projection of large-diameter fibers, whereas *area 1* receives a sparse projection of smaller fibers (Jones et al. 1970, 1982; Powell and Mountcastle 1959b).

These dipoles were placed in a spherical homogeneous volume-conductor model of the head (10-cm radius) to generate calculated waveforms and potential distributions (Darcey 1979). Surface potentials were calculated at 5-mm intervals on an 8 × 8 grid (Fig. 9*C*), simulating the location of the 64-electrode array over sensorimotor cortex (e.g., Fig. 1*A*). Potentials generated by the two dipoles were calculated separately and then summed according to the principle of superposition to produce the distributions and waveforms shown in Fig. 9, *C* and *D*.

Predicted distributions (Fig. 9*C*), and comparisons with representative empirical distributions (Fig. 1*C*), may be summarized as follows:

At 18 ms the calculated distribution is due almost entirely to the *area 3b* generator, because the primary positivity of *area 3b* is near its maximum, whereas the primary positivity of *area 1* is just beginning. The distribution has a shape corresponding to a tangential dipole, positive anterior to the CS (corresponding to the surface side of the primary positivity of *area 3b*) and negative posterior to it (corresponding to the white matter side of the dipole). The small contribution of the primary positivity of *area 1* at this latency produces a slight extension of positivity into the medial postcentral region. This distribution is similar to the empirical distributions of Fig. 1*C* at 20–22 ms.

At 22 ms the calculated distribution includes sizable contributions from both the *area 3b* and *area 1* generators and consists of an added region of positivity medial to the extrema of the *area 3b* distribution, representing a mixture of the primary positivities of *area 3b* and *area 1*. Unlike the *area 3b* distribution, only the surface or positive side of the *area 1* primary positivity is evident at the cortical surface because its major orientation is radial instead of tangential to the cortical surface. Compare with Fig. 1*C* at 23–24 ms.

At 25 ms the calculated distribution is due mainly to the primary positivity of *area 1* and the primary negativity of *area 3b* is just beginning and is prominent as the lateral extension of the positive maximum postcentrally and the region of weak negativity in the lateral precentral region. Compare with Fig. 1*C* at 26–28 ms.

At 30 ms the calculated distribution is due mainly to the *area 3b* primary negativity, and again approximates that produced by a tangential dipole, but with opposite polarity to the one at 18 ms. The slight extension of postcentral negativity is because of the small primary negativity of *area 1*. Compare with Fig. 1*C* at 32–33 ms.

At 35 ms the calculated distribution is due mainly to the primary negativity of *area 1* and is the converse of the one at 25 ms. The residual primary negativity of *area 3b* is evident as the lateral extension of the precental negativity and the region of weak positivity in the lateral postcentral region. Compare with Fig. 1*C* at 37–39 ms.

Predicted waveforms (Fig. 9*D*), and comparisons with empirical waveforms (Figs. 1*B*, 2*A*, and 3*A*), may be summarized as follows:

Positivities in the 20 to 30-ms latency range in the calculated waveforms show a progressive increase in latency from precentral to postcentral locations (Fig. 9*D*, *locations 25–32*), due to the superposition of the primary positivity of *area 3b* (P20), the primary positivity of *area 1* (P25), and the primary negativity of *area 3b* (P30) as recorded postcentrally. P20 contributes most of the voltage at precentral locations (e.g., *location 25*), P25 contributes most of the voltage at locations near the CS (*location 29*), and P30 contributes most of the voltage at postcentral locations (e.g., *location 32*). Intermediate locations (e.g., *location 30*) show intermediate latencies. These latency shifts thus reflect the temporal overlap of three distinct neurophysiological processes in a pair of generators with fixed location and orientation. These waveforms are similar to the empirical waveforms of Fig. 1*B* at *locations 27–30, 39*, and *56*, and Fig. 2*A* at *locations 6, 4*, and *1*.

The surface negativity in the 30 to 35-ms latency range shows a progressive increase in latency from precentral to postcentral locations (Fig. 9*D*, *locations 26–30*), similar to that seen in the empirical waveforms of Fig. 1*B* at *locations 36, 29*, and *7*, and Fig. 2*A* at *locations* just medial to *5*, and *4*. As in the previous example, this latency shift reflects a varying mixture of *area 3b* and *area 1* potentials.

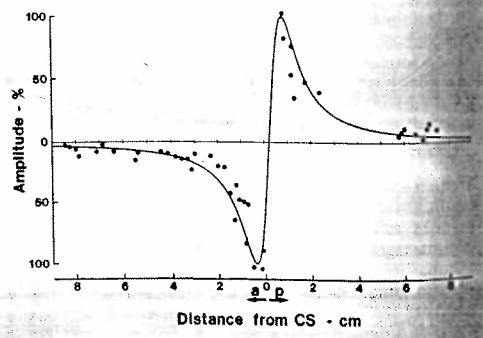


FIG. 10. Calculated and empirical distribution of cortical surface and intracerebral potential. Calculated distribution of potential (——) is as a function of distance anterior (a) and posterior (p) to the CS, with the use of the 2-dipole model illustrated in Fig. 9. Empirical amplitudes (○) were determined at 4 cortical surface and 3 intracerebral locations as described in the text.

Precentral locations near the CS exhibit waveforms of varying morphology in the 20 to 30-ms latency range, reflecting different mixtures of the *area 3b* and *area 1* primary positivites. For example, at *location 28* of Fig. 9*D*, P25 appears as an inflection on the falling phase of P20, similar to the empirical waveform of Fig. 1*B* at *location 37*, and Fig. 3*A* at *location 4*.

Medial postcentral locations may show little or no N20 (Fig. 9*D*, *location 29*) because of the superposition of the early portion of P25, similar to the empirical waveforms of Fig. 1*B* at *location 7* and Fig. 2 at *location 4*. Thus an initial negativity is indicative of a postcentral recording location and is a useful localizing criterion, but an initial positivity is not necessarily indicative of a precentral recording location (Wood et al. 1988).

This model of electrogenesis can also be used to predict the intracerebral distribution of potential (Fig. 10). The peak-to-peak amplitudes of P20–N30 and N20–P30 were measured in eight patients in whom both cortical-surface and depth-probe recordings were made. Cortical-surface amplitudes were measured from motor cortex, somatosensory cortex, and the gyri adjacent to them (e.g., Fig. 1, *locations 26, 36, 47*, and *56*, respectively). Intracerebral amplitudes were measured at frontal and occipital locations (e.g., Fig. 7, *locations LF 1, LFT 1*, and *LOT 3*). Analysis was based on the largest amplitude recorded within each region. Amplitudes were normalized to the value at somatosensory cortex and are indicated as dots in Fig. 10. The distance of electrode locations from the CS was determined by intraoperative photographs (surface recordings) and by lateral X-rays (depth-probe recordings) by the use of the mean location of the CS in the hand area (Fig. 8). This distribution of potential is similar to the calculated distribution (——), also normalized to the maximum over somatosensory cortex. Thus not only are the polarities of N20–P30 and P20–N30 consistent with an origin in *area 3b* as discussed above, but also the amplitude distribution within the brain bears a close quantitative correspondence to the predictions of the model.

In summary, the cortical surface and intracerebral distribution of potential is similar to that predicted by generators located in *areas 3b* and *1* of somatosensory cortex.

We thank R. Bartozzi, J. Jasiorkowski, M. Pearson, E. Roessler, and D. Thompson for assistance. Drs. R. Bucholz, W. F. Collins, III, P. Dickey, J. Partington, J. Piepmeier, and J. C. VanGilder collaborated in some recordings; and Drs. S. J. Jones and J. Wolpaw provided helpful reviews of previous versions of this paper.

This work was supported by the Veterans Administration and by National Institute of Mental Health Grant MH-05286.

Address for reprint requests: T. Allison, Neuropsychology Laboratory 116B1, V.A. Medical Center, West Haven, CT 06516.

Received 25 April 1988; accepted in final form 27 April 1989.

## REFERENCES

ALLISON, T. Scalp and cortical recordings of initial somatosensory cortex activity to median nerve stimulation in man. *Ann. NY Acad. Sci.* 388: 671–678, 1982.

ALLISON, T., GOFF, W. R., AND STERMAN, M. B. Cerebral somatosensory responses evoked during sleep in the cat. *Electroencephalogr. Clin. Neurophysiol.* 21: 461–468, 1966.

ALLISON, T., GOFF, W. R., WILLIAMSON, P. D., AND VANGILDER, J. C. On the neural origin of early components of the human somatosensory evoked potential. In: *Clinical Uses of Cerebral, Brainstem and Spinal Somatosensory Evoked Potentials. Progress in Clinical Neurophysiology, Volume 7*, edited by J. E. Desmedt. Basel: Karger, 1980, p. 51–68.

ALLISON, T., MCCARTHY, G., WOOD, C. C., GOFF, W. R., SPENCER, D. D., AND WILLIAMSON, P. D. SEPs recorded from the human cortical surface before and after resection of the somatosensory hand representation area (Abstract). *Electroencephalogr. Clin. Neurophysiol.* 58: 45 p, 1984.

ALLISON, T., MCCARTHY, G., WOOD, C. C., SPENCER, D. D., AND WILLIAMSON, P. D. Human cortical potentials evoked by stimulation of the median nerve. II. Cytoarchitectonic areas generating long-latency activity. *J. Neurophysiol.* 62: 711–722, 1989.

ALLISON, T., WOOD, C. C., AND MCCARTHY, G. Somatosensory evoked potentials following surgical excision of somatosensory or motor cortex in the monkey. *Soc. Neurosci. Abstr.* 12: 1432, 1986.

AREZZO, J., LEGATT, A. D., AND VAUGHAN, H. G., JR. Topography and intracranial sources of somatosensory evoked potentials in the monkey. I. Early components. *Electroencephalogr. Clin. Neurophysiol.* 46: 155–172, 1979.

AREZZO, J., VAUGHAN H. G., JR., AND LEGATT, A. D. Topography and intracranial sources of somatosensory evoked potentials in the monkey. II. Cortical components. *Electroencephalogr. Clin. Neurophysiol.* 51: 1–18, 1981.

BAILEY, P. AND VON BONIN, G. *The Isocortex of Man*. Urbana, IL: Univ. of Illinois Press, 1951.

BRAAK, H. *Architectonics of the Human Telencephalic Cortex*. Berlin: Springer-Verlag, 1980.

BROUGHTON, R. Discussion. In: *Average Evoked Potentials: Methods, Results and Evaluations*, edited by E. Donchin and D. B. Lindsley. Washington, DC: NASA, 1969, p. 79–84. (Publ. SP-191)

BROUGHTON, R., RASMUSSEN, T., AND BRANCH, C. Scalp and direct cortical recordings of somatosensory evoked potentials in man (circa 1967). *Can. J. Psychol.* 35: 136–158, 1981.

CELESIA, G. G. Somatosensory evoked potentials recorded directly from human thalamus and Sm I cortical area. *Arch. Neurol.* 36: 399–405, 1979.

CHIAPPA, K. H. *Evoked Potentials in Clinical Medicine*. New York: Raven, 1983.

CREUTZFELDT, O. AND HOUCHIN, J. Neuronal basis of EEG-waves. In: *Handbook of Electroencephalography and Clinical Neurophysiology*, 2C, edited by A. Remond. Amsterdam: Elsevier, 1974, p. 5–55.

DARCEY, T. M. *Methods for the Localization of Electrical Sources in the Human Brain and Applications to the Visual System* (Ph.D. Dissertation). Pasadena, CA: California Institute of Technology, 1979.

DEIBER, M. P., GIARD, M. H., AND MAUGUIÈRE, F. Separate generators with distinct orientations for N20 and P22 somatosensory evoked potentials to finger stimulation. *Electroencephalogr. Clin. Neurophysiol.* 65: 321–334, 1986.

DESMEDT, J. E. AND BOURGUET, M. Color imaging of parietal and frontal somatosensory potential fields evoked by stimulation of median or posterior tibial nerve in man. *Electroencephalogr. Clin. Neurophysiol.* 62: 1–17, 1985.

DESMEDT, J. E. AND CHERON, G. Noncephalic reference recording of early somatosensory potentials to finger stimulation in adult or aging normal man: differentiation of widespread N18 and contralateral N20 from the prerolandic P22 and N30 components. *Electroencephalogr. Clin. Neurophysiol.* 52: 553–570, 1981.

DEWEERD, A. W., LOOLENGA, A., VELDHUIZEN, R. J., AND VAN HUFFELEN, A. C. Somatosensory evoked potentials in minor cerebral ischemia: diagnostic significance and changes in serial records. *Electroencephalogr. Clin. Neurophysiol.* 62: 45–55, 1985.

DYKES, R. W. The anatomy and physiology of the somatic sensory cortical regions. *Prog. Neurobiol.* 10: 33–88, 1978.

GANDEVIA, S. C., BURKE, D., AND MCKEON, B. The projection of muscle afferents from the hand to cerebral cortex in man. *Brain* 107: 1–13, 1984.

GARDNER, E. P., HÄMÄLÄINEN, H. A., WARREN, S., DAVIS, J., AND YOUNG, W. Somatosensory evoked potentials (SEPs) and cortical single unit response elicited by mechanical tactile stimuli in awake monkeys. *Electroencephalogr. Clin. Neurophysiol.* 58: 537–552, 1984.

GOLDRING, S., ARAS, E., AND WEBER, P. C. Comparative study of sensory input to motor cortex in animals and man. *Electroencephalogr. Clin. Neurophysiol.* 29: 537–550, 1970.

HALONEN, JONES, S., AND SHAWKAT, F. Contribution of cutaneous and muscle afferent fibres to cortical SEPs following median and radial nerve stimulation in man. *Electroencephalogr. Clin. Neurophysiol.* 71: 331–335, 1988.

IWAMURA, Y., TANAKA, M., AND HIKOSAKA, O. Overlapping representation of fingers in the somatosensory cortex (area 2) of the conscious monkey. *Brain Res.* 197: 516–520, 1980.

JONES, E. G. The nature of the afferent pathways conveying short-latency inputs to primate motor cortex. In: *Motor Control Mechanisms in Health and Disease*, edited by J. E. Desmedt. New York: Raven, 1983, p. 263–285.

JONES, E. G., FRIEDMAN, D. P., AND HENDRY, S. H. C. Thalamic basis of place- and modality-specific columns in monkey somatosensory cortex: a correlative anatomical and physiological study. *J. Neurophysiol.* 48: 545–568, 1982.

JONES, E. G. AND POWELL, T. P. S. Connexions of the somatic sensory cortex of the rhesus monkey. III. Thalamic connexions. *Brain* 93: 37–56, 1970.

JONES, S. J. AND POWER, C. N. Scalp topography of human somatosensory evoked potentials: the effect of interfering tactile stimulation applied to the hand. *Electroencephalogr. Clin. Neurophysiol.* 58: 25–36, 1984.

JULIANO, S. L., FRIEDMAN, D. P., AND ESLIN, D. Patterns of cortico-cortical connectivity can predict patches of stimulus-evoked metabolic activity in monkey somatosensory cortex. *Soc. Neurosci. Abstr.* 13: 470, 1987.

JULIANO, S. L. AND WHITSEL, B. L. Metabolic labeling associated with index finger stimulation in monkey SI: between animal variability. *Brain Res.* 342: 242–251, 1985.

KAAS, J. H., SUR, M., NELSON, R. J., AND MERZENICH, M. M. The postcentral somatosensory cortex. In: *Cortical Sensory Organization. Multiple Representations of the Body in Primates*, edited by C. N. Woolsey. Clifton, NJ: Humana, 1981, vol. 1, p. 29–45.

KAUKORANTA, E., HÄMÄLÄINEN, M., SARVAS, J., AND HARI, R. Mixed and sensory nerve stimulations activate different cytoarchitectonic areas in the human primary somatosensory cortex SI. *Exp. Brain Res.* 63: 60–66, 1986.

KELLY D. L., JR., GOLDRING, S., AND O'LEARY, J. L. Averaged evoked somatosensory responses from exposed cortex of man. *Arch. Neurol.* 13: 1–9, 1965.

KULICS, A. T. AND CAULLER, L. J. Cerebral cortical somatosensory evoked responses, multiple unit activity and current source-densities: their interrelationships and significance to somatic sensation as revealed by stimulation of the awake monkey's hand. *Exp. Brain Res.* 62: 46–60, 1986.

LANDAU, W. M. Evoked potentials. In: *The Neurosciences*, edited by G. C. Quarton, T. Melnechuk, and F. O. Schmitt. New York: Rockefeller Univ. Press, 1967, p. 469–482.

LEMON, R. N. AND VAN DER BURG, J. Short-latency peripheral inputs to thalamic neurones projecting to the motor cortex in the monkey. *Exp. Brain Res.* 36: 445–462, 1979.

LLINÁS, R. AND NICHOLSON, C. Analysis of field potentials in the central nervous system. In: *Handbook of Electroencephalography and Clinical Neurophysiology*, 2B, edited by A. Remond. Amsterdam: Elsevier, 1974, p. 61–83.

LUEDERS, H., DINNER, D. S., LESSER, R. P., AND MORRIS, H. H. Evoked potentials in cortical localization. *J. Clin. Neurophysiol.* 3: 75–84, 1986.

LUEDERS, H., LESSER, R. P., HAHN, J., DINNER, D. S., AND KLEM, G. Cortical somatosensory evoked potentials in response to hand stimulation. *J. Neurosurg.* 58: 885–894, 1983.

MAUGUIÈRE, F., DESMEDT, J. E., AND COURJON, J. Astereognosis and dissociated loss of frontal or parietal components of somatosensory evoked potentials in hemispheric lesions. *Brain* 106: 271–311, 1983.

MITZDORF, U. Current source-density method and application in cat cerebral cortex: investigation of evoked potentials and EEG phenomena. *Physiol. Rev.* 65: 37–100, 1985.

NICHOLSON, C. AND FREEMAN, J. A. Theory of current source-density analysis and determination of conductivity tensor for Anuran cerebellum. *J. Neurophysiol.* 38: 356–368, 1975.

PAPAKOSTOPOULOS, D. AND CROW, H. J. The precentral somatosensory evoked potential. *Ann. N.Y. Acad. Sci.* 425: 256–261, 1984.

PERL, E. R. AND WHITLOCK, G. Potentials evoked in cerebral somatosensory region. *J. Neurophysiol.* 18: 486–501, 1955.

PONS, T. P. AND KAAS, J. H. Connections of area 2 of somatosensory cortex with the anterior pulvinar and subdivisions of the ventroposterior complex in Macaque monkeys. *J. Comp. Neurol.* 240: 16–36, 1985.

POWELL, T. P. S. AND MOUNTCASTLE, V. B. The cytoarchitecture of the postcentral gyrus of the monkey *Macaca mulatta*. *Bull. Johns Hopkins Hosp.* 105: 108–131, 1959a.

POWELL, T. P. S. AND MOUNTCASTLE, V. B. Some aspects of the functional organization of the cortex of the postcentral gyrus of the monkey: a correlation of findings obtained in a single unit analysis with cytoarchitecture. *Bull. Johns Hopkins Hosp.* 105: 133–162, 1959b.

SCHADY, W., OCHOA, J. L., TOREBJORK, H. E., AND CHEN, L. S. Peripheral projections of fascicles in the human median nerve. *Brain* 106: 745–760, 1983.

SCHLAG, J. Generation of brain evoked potentials. In: *Bioelectric Recording Techniques. Cellular Processes and Brain Potentials*, edited by R. F. Thompson and M. M. Patterson. New York: Academic, 1973, part A, p. 273–316.

SLIMP, J. C., TAMAS, L. B., STOLOV, W. C., AND WYLER, A. R. Somatosensory evoked potentials after removal of somatosensory cortex in man. *Electroencephalogr. Clin. Neurophysiol.* 65: 111–117, 1986.

SPENCER, S. S., SPENCER, D. D., WILLIAMSON, P. D., AND MATTSON, R. H. The localizing value of depth electroencephalography in 32 refractory epileptic patients. *Ann. Neurol.* 12: 248–253, 1982.

STOHR, P. E. AND GOLDRING, S. Origin of somatosensory evoked scalp responses in man. *J. Neurosurg.* 31: 117–127, 1969.

SUNDERLAND, S. AND BEDBROOK, G. M. The cross-sectional area of peripheral nerve trunks occupied by the fibres representing individual muscular and cutaneous branches. *Brain* 72: 613–624, 1949.

TALAIRACH, J. AND SZIKLA, G. *Atlas of Stereotaxic Anatomy of the Telencephalon*. Paris: Masson, 1967.

TOWE, A. L. On the nature of the primary evoked response. *Exp. Neurol.* 15: 113–139, 1966.

VOGT, M. Über omnilaminäre Strukturdifferenzen und lineare Grenzen der architektonischen Felder der hinteren Zentralwindung des Menschen. *J. Psychol. Neurol.* 35: 177–193, 1928.

WERNER, G. AND WHITSEL, B. L. Functional organization of the somatosensory cortex. In: *Handbook of Sensory Physiology. Somatosensory System*, edited by A. Iggo. Berlin: Springer-Verlag, 1973, vol. 2, p. 621–700.

WIESENDANGER, M. Input from muscle and cutaneous nerves of the hand and forearm to neurones of the precentral gyrus of baboons and monkeys. *J. Physiol.* 228: 203–219, 1973.

WOOD, C. C. AND ALLISON, T. Interpretation of evoked potentials: a neurophysiological perspective. *Can. J. Psychol.* 35: 113–135, 1981.

WOOD, C. C., ALLISON, T., MCCARTHY, G., SPENCER, D. D., AND WILLIAMSON, P. D. Somatosensory evoked potentials following surgical excision of human somatosensory or motor cortex. *Soc. Neurosci. Abstr.* 12: 1432, 1986.

WOOD, C. C., COHEN, D., CUFFIN, B. N., YARITA, M., AND ALLISON, T. Electrical sources in human somatosensory cortex: identification by combined magnetic and potential recordings. *Science Wash. DC* 227: 1051–1053, 1985.

WOOD, C. C., SPENCER, D. D., ALLISON, T., MCCARTHY, G., WILLIAMSON, P. D., AND GOFF, W. R. Localization of human sensorimotor cortex during surgery by cortical surface recordings of somatosensory evoked potentials. *J. Neurosurg.* 68: 99–111, 1988.

WOOLSEY, C. N. AND FAIRMAN, D. Contralateral, ipsilateral, and bilateral representation of cutaneous receptors in somatic areas I and II of the cerebral cortex of pig, sheep, and other mammals. *Surgery St. Louis* 19: 684–702, 1946.

YAMADA, T., KAYAMORI, R., KIMURA, J., AND BECK, D. O. Topography of somatosensory evoked potentials after stimulation of the median nerve. *Electroencephalogr. Clin. Neurophysiol.* 59: 29–43, 1984.

ZIMMERMAN, I. D. A triple representation of the body surface in the sensorimotor cortex of the squirrel monkey. *Exp. Neurol.* 20: 415–431, 1968.

# Human Cortical Potentials Evoked by Stimulation of the Median Nerve. II. Cytoarchitectonic Areas Generating Long-Latency Activity

TRUETT ALLISON, GREGORY MCCARTHY, CHARLES C. WOOD, PETER D. WILLIAMSON, AND DENNIS D. SPENCER

*Neuropsychology Laboratory, Veterans Administration Medical Center, West Haven, 06516; and Department of Neurology and Section of Neurosurgery, Yale University School of Medicine, New Haven, Connecticut 06520*

## SUMMARY AND CONCLUSIONS

*1.* The anatomic generators of human median nerve somatosensory evoked potentials (SEPs) in the 40 to 250-ms latency range were investigated in 54 patients by means of cortical-surface and transcortical recordings obtained during neurosurgery.

*2.* Contralateral stimulation evoked three groups of SEPs recorded from the hand representation area of sensorimotor cortex: P45-N80-P180, recorded anterior to the central sulcus (CS) and maximal on the precentral gyrus; N45-P80-N180, recorded posterior to the CS and maximal on the postcentral gyrus; and P50-N90-P190, recorded near and on either side of the CS.

*3.* P45-N80-P180 inverted in polarity to N45-P80-N180 across the CS but was similar in polarity from the cortical surface and white matter in transcortical recordings. These spatial distributions were similar to those of the short-latency P20–N30 and N20–P30 potentials described in the preceding paper, suggesting that these long-latency potentials are generated in *area 3b* of somatosensory cortex.

*4.* P50-N90-P190 was largest over the anterior one-half of somatosensory cortex and did not show polarity inversion across the CS. This spatial distribution was similar to that of the short-latency P25–N35 potentials described in the preceding paper and, together with our and Goldring et al. 1970; Stohr and Goldring 1969 transcortical recordings, suggest that these long-latency potentials are generated in *area 1* of somatosensory cortex.

*5.* SEPs of apparently local origin were recorded from several regions of sensorimotor cortex to stimulation of the ipsilateral median nerve. Surface and transcortical recordings suggest that the ipsilateral potentials are generated not in *area 3b*, but rather in other regions of sensorimotor cortex perhaps including *areas 4, 1, 2,* and *7*. This spatial distribution suggests that the ipsilateral potentials are generated by transcallosal input from the contralateral hemisphere.

*6.* Recordings from the periSylvian region were characterized by P100 and N100, recorded above and below the Sylvian sulcus (SS) respectively. This distribution suggests a tangential generator located in the upper wall of the SS in the second somatosensory area (SII). In addition, N125 and P200, recorded near and on either side of the SS, suggest a radial generator in a portion of SII located in surface cortex above the SS.

*7.* In comparison with the short-latency SEPs described in the preceding paper, the long-latency potentials were more variable and were more affected by intraoperative conditions.

## INTRODUCTION

The preceding paper (Allison et al. 1989) described median nerve somatosensory evoked potentials (SEPs) recorded from the contralateral sensorimotor cortex in the 20 to 40-ms latency range, and presented a model for their generators involving asynchronous activation of cytoarchitectonic *areas 3b* and *1* of somatosensory cortex. In this paper we first consider similarly recorded SEPs in the 40 to 250-ms latency range. The same model proposed for the short-latency potentials is useful in characterizing the long-latency potentials, provides a reasonable account of many of their spatiotemporal features, and suggests that these potentials are also generated in *areas 3b* and *1*.

Other regions of sensorimotor cortex, and the second somatosensory area, appear to generate long-latency SEPs to contralateral and ipsilateral stimulation. Although the intraoperative conditions in which these recordings were obtained probably provide an incomplete sample of long-latency cortical potentials evoked by median nerve stimuli, this study provides the first detailed description of SEPs recorded directly from human sensorimotor and periSylvian cortex. Unless noted otherwise, all human and animal potentials discussed in this paper were evoked by electrical stimulation of the contralateral median nerve at the wrist.

## METHODS

Methods of stimulating and recording were described previously (Allison et al. 1989; Wood et al. 1988). In 18 patients operated under local anesthesia (with administration of fentanyl and droperidol) the recording epoch was 490 ms, and a long interstimulus interval (2.5 s) was used. In 36 patients operated under general endotracheal anesthesia (thiopental sodium during intubation, followed by 40–60% nitrous oxide and 0.3–1.0% isoflurane in oxygen), shorter interstimulus intervals (0.4–0.6 s) and a shorter recording epoch (128 ms) were used. Two to four averages ($n$ = 32 or 48) were obtained to determine SEP variability. The protocols used in this study were approved by the Human Investigation Committees of the West Haven VA Medical Center and Yale University School of Medicine. Informed consent was obtained.

## RESULTS

### *Surface recordings from contralateral sensorimotor cortex*

The surface distribution of long-latency potentials over sensorimotor cortex is illustrated in Fig. 1, which shows topographic maps of root mean square (RMS, a measure of total amplitude independent of waveform morphology and polarity) voltage for four patients in whom a 64-electrode

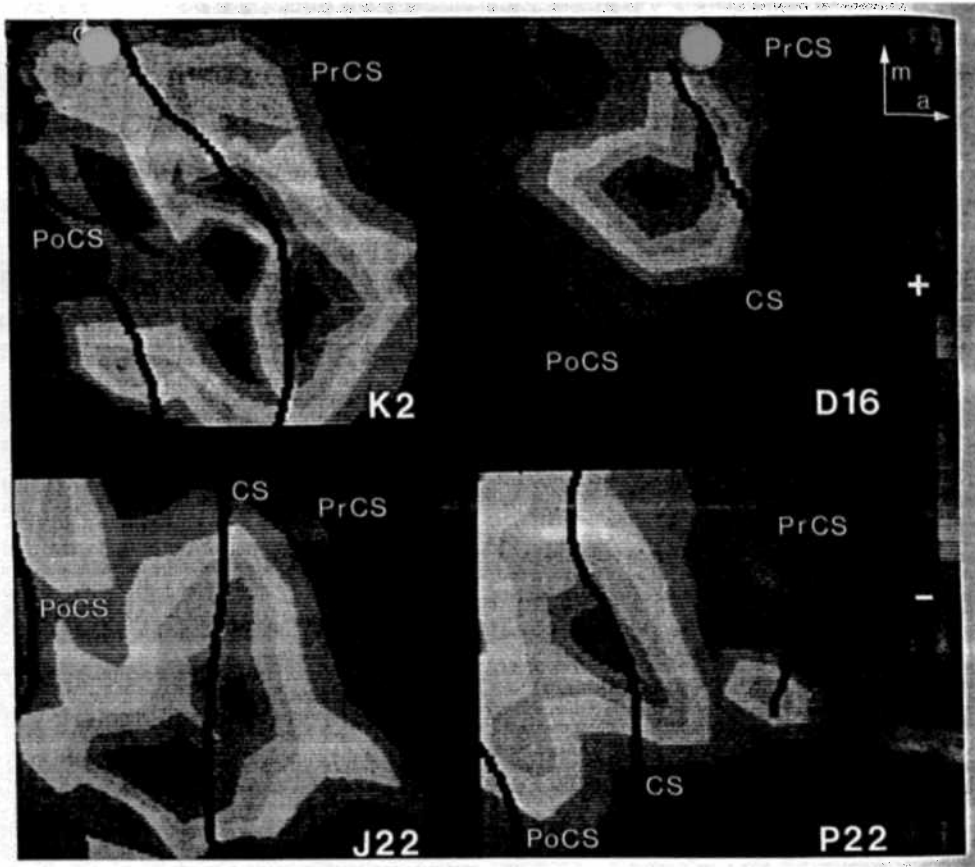


FIG. 1. Topography of root mean square (RMS) voltage in the 40 to 108-ms latency range in relation to the anatomy of sensorimotor cortex in 4 patients. *Patients K2* and *P22*, right frontal lobe epileptogenic region distant from sensorimotor cortex; *D16* and *J22*, right frontal lobe astrocytoma distant from sensorimotor cortex; general anesthesia in all cases. RMS values are positive and hence are in the green-red side of the color scale; each color represents ⅛ the total RMS voltage in each patient. In this and following figures, CS, central sulcus; PoCS, postcentral sulcus; PrCS, precentral sulcus. In this and Fig. 5*D*, sulci are superimposed on maps based on recordings using the 64-electrode array; each map encompasses an area 35 × 35 mm; maps constructed as in the preceding paper (Allison et al. 1989).

array (see Fig. 1*A* of the preceding paper) was well positioned to record from the high-amplitude region. In every case largest amplitudes were obtained over sensorimotor cortex near the central sulcus (CS). This distribution is similar to the RMS topography of short-latency SEPs (Wood et al. 1988) but with relatively more precentral voltage in some cases. In some patients operated under local anesthesia, the frontal lobe was explored well anterior to motor cortex; focal potentials indicative of local origin were not recorded. With the exception of recordings near the Sylvian sulcus (see below), recordings from parietal and temporal cortex showed, if anything, smaller potentials similar to those recorded from somatosensory cortex, suggesting that they were not locally generated. However, the possibility that some portion of the activity recorded outside sensorimotor and periSylvian cortex is generated locally cannot be ruled out. In nine cases small-amplitude potentials were recorded that had no clear spatiotemporal pattern or steep voltage gradients and could not be characterized except to say that they were largest over sensorimotor cortex.

Figure 2 compares long-latency SEPs recorded from the cortical surface with the short-latency potentials described previously (Allison et al. 1989; Wood et al. 1988). From

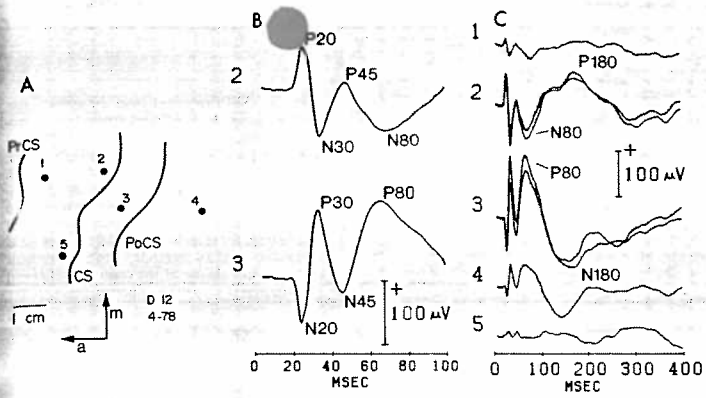


FIG. 2. SEPs recorded from the cortical surface. *A: patient D12*; left frontal lobe glioma impinging on hand area of motor cortex; local anesthesia. *B*: shorter-latency SEPs. *C*: long-latency SEPs from locations shown in *B* and from additional locations outside the region of high-amplitude potentials. Representative between-average variability in this and other recordings is shown at *locations 2* and *3*; all other tracings are the mean of the individual averages. In this and following figures, positive voltage upward; stimulus delivered at 0 ms, stimulus artifact not shown.

motor cortex (*location 2*) P20–N30 was followed by a positive potential at about 45 msec (P45) and a negativity (N80), and from somatosensory cortex (*location 3*) N20–P30 was followed by N45 and P80 potentials (Fig. 1*B*). These, in turn, were followed by precentral P180 and postcentral N180 potentials (Fig. 1*C*). Thus this activity was characterized by a sequence of potentials of increasing latency and duration, but of opposite polarity as recorded from motor and somatosensory cortex; that is, the precentral and postcentral waveforms showed a polarity inversion across the CS. The later potentials were largest at the same locations where the earlier potentials were largest (*locations 2* and *3* in this recording), and were smaller anterior (*location 1*), posterior (*location 4*) and lateral (*location 5*) to the hand area of sensorimotor cortex. We will refer to the P45-N80-P180 and N45-P80-N180 sequences as the "precentral" and "postcentral" potentials respectively. The polarity-latency nomenclature used to label these and other potentials is based on approximate mean peak latencies across patients (Table 1). Recordings like those of Fig. 2, in which only the precentral and postcentral potentials were clearly observed, were obtained in seven cases.

In eight cases, of which Fig. 3 is an example, a different spatiotemporal pattern of activity was recorded. P25–N35 (Allison et al. 1989; Wood et al. 1988) was followed by a positivity at ~50 ms (P50), a negativity (N90), and positivity (P190). This P50-N90-P190 sequence was usually largest where P25–N35 was largest. In recordings with good coverage of the entire hand area of sensorimotor cortex, these potentials were largest over the medial and central hand area of somatosensory cortex. In the recording of Fig. 3, there were no medial recording sites on somatosensory cortex, and the largest P25-N35-P50-N90-P190 sequence was recorded from a precentral site (*location 3*) near the CS. Like P25, P50-N90-P190 did not show polarity inversion or sharp voltage gradients across the CS. For example, precentral *location 2* recorded P20–N30, while postcentral *location 4* recorded N20–P30; in contrast, the longer-latency potentials were similar in waveform at both locations. Since P50-N90-P190 was largest near the CS and

TABLE 1. *Long-latency SEPs summarized*

| | Latency or Amplitude | | | | | | | | | | | | | | | |
|---|---|---|---|---|---|---|---|---|---|---|---|---|---|---|---|---|
| | P45 Lat, ms | N80 Lat, ms | P180 Lat, ms | P45-N80 Amp, μV | N80-P180 Amp, μV | N45 Lat, ms | P80 Lat, ms | N180 Lat, ms | N45-P80 Amp, μV | P80-N180 Amp, μV | P50 Lat, ms | N90 Lat, ms | P190 Lat, ms | P50-N90 Amp, μV | N90-P190 Amp, μV |
| Anesthesia | | | | | | | | | | | | | | | |
| Local | 47.3 | 82.6 | 179.2 | 60.4 | 100.8 | 46.5 | 84.3 | 180.8 | 99.0 | 149.1 | 52.8 | 91.2 | 181.0 | 110.2 | 140.9 |
| | ± 1.6 | ± 4.7 | ± 7.4 | ± 9.6 | ± 17.9 | ± 2.0 | ± 4.1 | ± 8.3 | ± 19.5 | ± 28.1 | ± 2.0 | ± 4.9 | ± 6.8 | ± 20.4 | ± 19.7 |
| | (15) | (14) | (12) | (14) | (11) | (15) | (15) | (12) | (15) | (13) | (11) | (11) | (10) | (11) | (10) |
| General | 49.5 | 87.2 | 170.0 | 56.3 | 58.8 | 46.4 | 84.0 | 159.0 | 59.4 | 83.0 | 56.0 | 98.9 | 188.3 | 121.6 | 88.3 |
| | ± 1.4 | ± 2.6 | ± 11.1 | ± 7.1 | ± 23.7 | ± 1.4 | ± 2.8 | ± 7.8 | ± 9.1 | ± 28.2 | ± 1.4 | ± 2.2 | ± 6.0 | ± 17.3 | ± 61.0 |
| | (24) | (23) | (5)* | (23) | (4)* | (24) | (23) | (5)* | (22) | (5)* | (26) | (25) | (3)* | (25) | (3)* |
| Total | 48.6 | 85.4 | 176.5 | 57.8 | 89.6 | 46.4 | 84.1 | 174.4 | 75.5 | 130.7 | 55.1 | 96.6 | 182.7 | 118.1 | 128.8 |
| | ± 1.0 | ± 2.4 | ± 6.0 | ± 5.7 | ± 15.0 | ± 1.2 | ± 2.3 | ± 6.6 | ± 9.9 | ± 22.5 | ± 1.1 | ± 2.2 | ± 5.4 | ± 13.4 | ± 20.2 |
| | (39) | (37) | (17) | (37) | (15) | (39) | (38) | (17) | (37) | (18) | (37) | (36) | (13) | (36) | (13) |

Values are means ± SE; nos. in parentheses are no. of patients. SEPs, somatosensory evoked potentials. *See text.

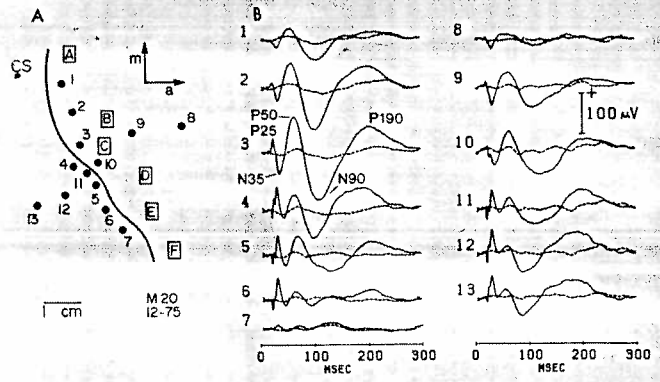


FIG. 3. SEPs recorded from the cortical surface. *A: patient M20*; right orbitofrontal epileptogenic region; local anesthesia. Cortical stimulation: A, leg and toe flexion; B, flexion of fingers; C, wrist movement; D, forearm flexion; E, neck extension; F, mouth movement. In this and following figures, sensory and motor responses to cortical stimulation refer to contralateral side of body except for speech-related and some perioral responses. *B*: SEPs recorded from sensorimotor cortex to stimulation of the contralateral (——) or ipsilateral (– – –) median nerve.

recorded on either side of it, this pattern of activity will be referred to as the "periCS" potentials. The periCS potentials were largest in the hand area of sensorimotor cortex and were smaller medial (*location 1*), lateral (*location 6*), anterior (*location 8*), and posterior (*location 13*) to it.

The peak-to-peak amplitudes and peak latencies of these potentials are summarized in Table 1. As was the case for short-latency SEPs (Allison et al. 1989), long-latency potentials were in most cases smaller in amplitude under general as compared with local anesthesia (Table 1), but because of large variability the differences were not significant. Table 1 appears to indicate that potentials later than 100 ms were often abolished by general anesthesia (indicated by asterisks), but this is artifactual because, in most patients operated under general anesthesia, the recording epoch was only 108 ms. SEPs were not significantly affected by the location or type of pathology (not shown in Table 1), suggesting that these variables did not have a systematic effect on the results.

The precentral and postcentral potentials, and the periCS potentials, appeared to be recordable in relative isolation in some cases and had different spatiotemporal characteristics. However, in most cases both types of activity were recorded. Figure 4 is an example; from *location 1* the precentral P20-N30-P45-N80 potentials were recorded, and from *location 2* the postcentral N20-P30-N45-P80 potentials were recorded (Fig. 4*B*). From a postcentral site (*location 3*) near the CS a different waveform was seen, consisting of a small P25–N35, followed by P50, which was typically ~5 ms later than N45–P45. P50 was followed by N90, which was typically ~10 ms later than N80–P80. From precentral *location 1*, P50 was seen as a positive inflection (Fig. 4*B*, *) on the falling phase of P45, and N90 was seen as a negative deflection (Fig. 4*C*, *) after N80. As in Fig. 3, P50 and N90 were recorded at the same polarity near the CS and on either side of it, and all potentials were small medial (*location 4*), anterior (*location 5*), and lateral (*location 6*) to the hand area.

Figure 5 shows another recording in which both types of activity were seen. The P45–N80 precentral potentials were recorded from *location 27*, and the N45–P80 postcentral potentials were recorded from *location 53*. From the me-

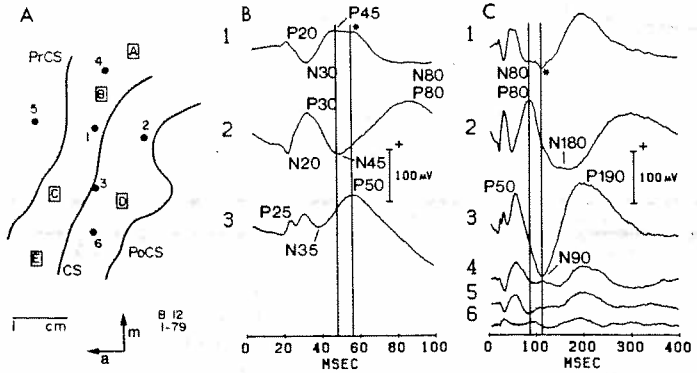


FIG. 4. SEPs recorded from the cortical surface. *A: patient B12*; left frontal lobe epileptogenic region distant from sensorimotor cortex; local anesthesia. Cortical stimulation: A, leg flexion; B, forearm and hand movement; C, jaw movement; D, tingling of 1st digit; E, mouth movement. *B*: shorter-latency SEPs. Isolatency lines are at the peak of P45–N45 (48 ms) and the peak of P50 (56 ms). *C*: long-latency SEPs recorded from locations in *B* and from additional locations (*4–6*) outside the hand area. Isolatency lines are at the peak of N80–P80 (84 ms) and the peak of N90 (112 ms).



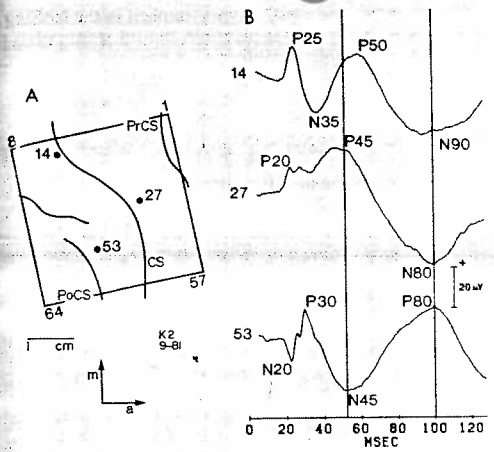


FIG. 5. SEPs recorded from the cortical surface. *A: patient K2*; right frontal lobe epileptogenic region distant from sensorimotor cortex; general anesthesia. Rectangle indicates placement of the 64-electrode array and hence the region encompassed by the topographic maps in *D*. *B*: SEPs at selected locations. Isolatency lines at the approximate peaks of P45–N45 (52 ms) and N80–P80 (100 ms). *C*: SEPs at each location of the 64-electrode array. Isolatency lines as in *B*. *D*: isovoltage contour maps at 23, 55, and 100 ms.

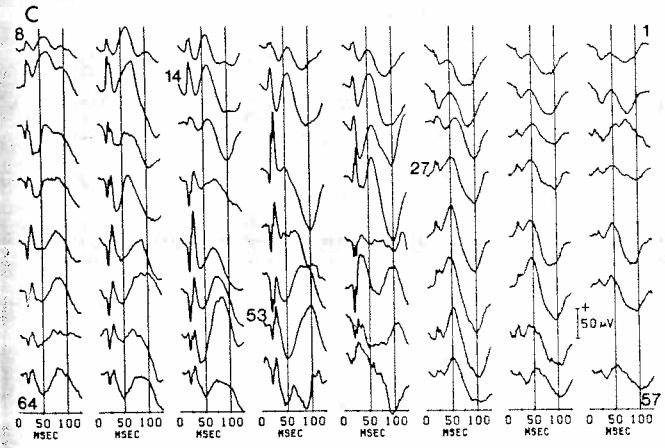

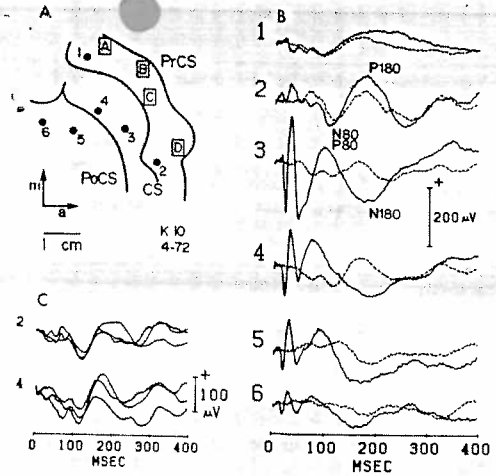


FIG. 6. SEPs recorded from the cortical surface. *A: patient K10*; right parietal lobe epileptogenic region in the face area of somatosensory cortex; local anesthesia. Cortical stimulation: A, arm abduction; B, forearm flexion; C, hand flexion; D, eyelid and neck movement. *B*: SEPs to stimulation of the contralateral (——) or ipsilateral (– – –) median nerve. *C*: representative between-average variability of ipsilateral SEPs.

dial portion of the hand area, P50 was separable both spatially and temporally from N45–P45. However, N90 was not distinguishable from N80 by peak latency either in the selected waveforms of Fig. 5*B* or the complete set of waveforms in Fig. 5*C*. Figure 5*C* also demonstrates the complexity of long-latency SEPs seen in some cases. In this recording the parcellation of potentials into the precentral and postcentral, and peri types (implicit in the labeling of potentials in Fig. 5*B*) is plausible, but other interpretations of these complex waveforms are possible.

Figure 5*D* shows isovoltage topographic maps of this activity. The distribution of potential at 23 ms will be described first for comparison with the long-latency distributions. At the peak of N20–P20 and 3 ms before the peak of P25, the distribution consists of a lateral precentral maximum corresponding to P20, a lateral postcentral minimum corresponding to N20, and a medial postcentral maximum corresponding to P25; this distribution is similar to those described previously (Allison et al. 1989; Wood et al. 1988). At 55 ms the distribution consists of a lateral precentral maximum corresponding to P45, a lateral postcentral minimum corresponding to N45, and a medial postcentral maximum corresponding to P50. Note the similarity of this distribution to the one at 23 ms. At 100 ms N80–P80 is seen as a precentral minimum and a postcentral maximum in the lateral portion of the map, and an additional minimum is seen near the CS in the central portion of the map. The latter minimum corresponds to the N90 distribution, but is more lateral than the P25 and P50 distributions. N80 and N90 were spatially distinct, although, as noted above, they were not temporally distinct in this case. A recording epoch of 108 ms was used in this case, hence topographic maps of P180, N180, and P190 were not obtained. However, recordings using a 490-ms epoch (e.g., Figs. 2 and 3) indicate that their distributions were similar to those of P45, N45, and P50, respectively.

To summarize, the precentral and postcentral potentials, and the periCS potentials, could occasionally be recorded in relative isolation, but in most cases long-latency SEPs appeared to be a mixture of both types of potentials. The precentral potentials had spatial distributions similar to those of P20–N30, and, likewise, the postcentral potentials had distributions similar to those of N20–P30. In general the periCS potentials had distributions similar to those of

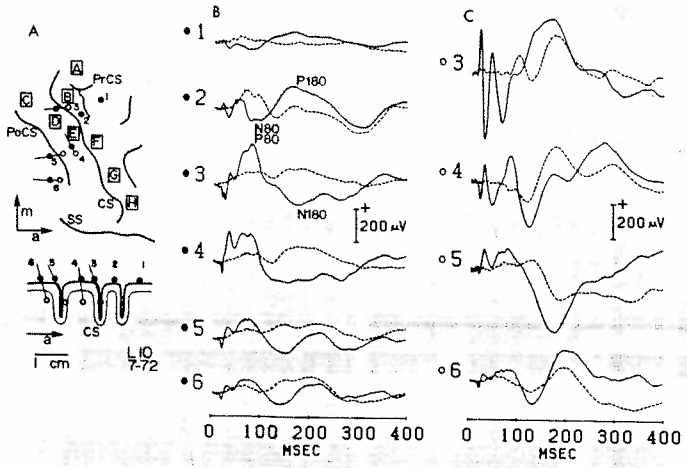


FIG. 7. Transcortical recordings of SEPs. *A: patient L10*; right frontal lobe epileptogenic region distant from sensorimotor cortex; local anesthesia. Cortical stimulation: A, shoulder movement; B, arm movement; C, hand movement; D, 3rd digit movement; E, 1st digit movement; F, head and back movement; G, mouth movement; H, jaw and throat movement. (In this patient stimulation of somatosensory or motor cortex evoked only motor responses). In this and Fig. 8, the *bottom drawing* is a schematic quasi-sagittal view of locations of surface (●) and estimated locations of deep (○) electrodes of the transcortical pairs. SS, Sylvian sulcus. *B*: SEPs recorded from the cortical surface to stimulation of the contralateral (——) or ipsilateral (– – –) median nerve. *C*: SEPs recorded from deep locations to stimulation of the contralateral (——) or ipsilateral (– – –) median nerve.



P25–N35, but they were often we corded from more lateral locations in the hand area near the CS as well.

*Surface recordings from ipsilateral sensorimotor cortex*

In 13 patients cortical surface recordings were also obtained to stimulation of the ipsilateral median nerve. No short-latency potentials to ipsilateral stimulation were seen in any recording (Allison et al. 1989; Wood 1988), nor could definite long-latency potentials be recorded in eight patients (e.g., Fig. 3). However, in five cases evidence of ipsilateral long-latency activity was seen. Figure 6*B* compares SEPs recorded at the same locations with contralateral and ipsilateral stimulation. To contralateral stimulation, N80–P180 and P80–N180 were recorded respectively from precentral (*location 2*) and postcentral (*location 3*) sites in the lateral part of the hand area. By contrast, the ipsilateral potentials did not change polarity across the CS. Rather, polarity inversions were recorded from sites posterior (*locations 5* and *6*) to the postcentral sulcus (PoCS) compared to sites anterior to it (*locations 1–4*). The ipsilateral potentials did not have a sharp onset in this and other recordings, but onset latency was ~40–50 ms. They were largest in the same general region from which the largest contralateral activity was recorded, although their amplitude was smaller than the contralateral potentials in this and other recordings. They tended to be more variable than the contralateral potentials but were clearly reproducible (Fig. 6*C*).

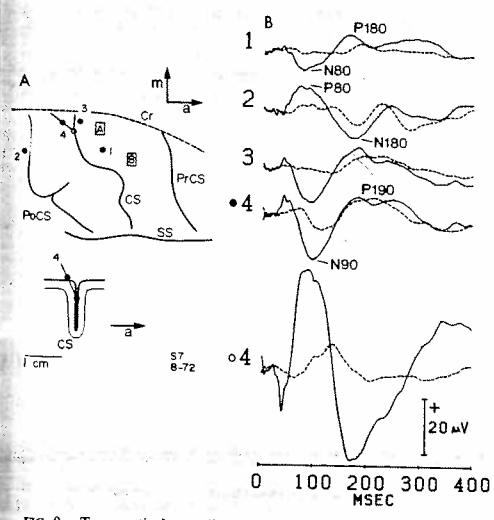


FIG. 8. Transcortical recordings of SEPs. *A: patient S7*; right temporal lobe calcified mass; local anesthesia. Cortical stimulation: A, hand and mouth movement; B, mouth movement. Cr, medial margin of craniotomy. *B*: SEPs evoked by stimulation of the contralateral (——) or ipsilateral (– – –) median nerve.

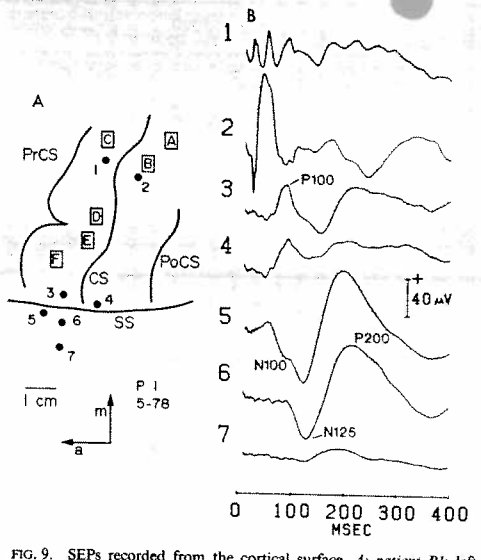


FIG. 9. SEPs recorded from the cortical surface. *A: patient P1*; left frontal lobe astrocytoma distant from sensorimotor and periSylvian cortex; local anesthesia. Cortical stimulation: A, arm numbness; B, arm movement; C, hand movement; D, throat movement; E, face movement; F, speech arrest. *B*: Recordings from the hand area of sensorimotor cortex (*locations 1* and *2*), and from periSylvian cortex (*locations 3–7*).

*Transcortical recordings from sensorimotor cortex*

Transcortical recordings were obtained in five patients (Allison et al. 1989) and provided additional information regarding the surface and intracerebral distribution of potential. Figure 7*B* shows surface recordings to contralateral and ipsilateral stimulation. To contralateral stimulation the N80–P180 precentral (*location 2*) and P80–N180 postcentral (*location 3*) potentials were recorded, similar to the surface recordings described above. Ipsilateral potentials were small and similar at all locations except for 80 to 100-ms positive potentials recorded from motor cortex (*location 2*).

Deep recordings (Fig. 7*C*) showed a polarity inversion of P20-N30-P45 at precentral *location 3* to N20-P30-N45 at postcentral *location 4*. There was weak evidence of N80–P80 (at ~65 ms) and P180–N180 (at ~135 ms), but the waveforms in this latency range were complex and suggested the presence of additional activity. In contrast, the ipsilateral potentials recorded from these locations showed similar waveforms. *Electrode 3* deep was probably located on or anterior to the surface of the posterior wall of the CS, thus *electrodes 3* deep and *4* deep constituted a transcortical recording across the cortex of the posterior wall of the CS. Recordings from deep electrodes spanning the PoCS (*locations 4–6*) showed marked changes in waveform and steep voltage gradients of the contralateral and ipsilateral potentials.

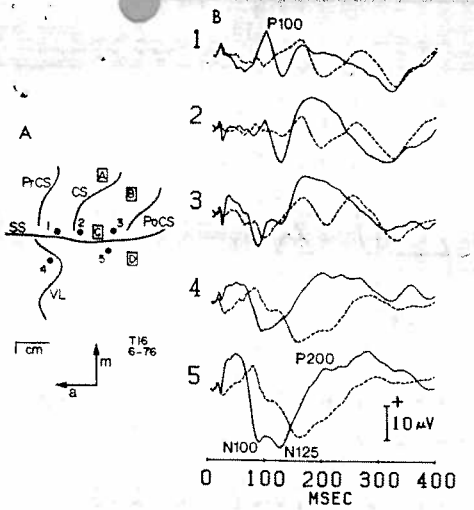


FIG. 10. SEPs recorded from periSylvian cortex. *A: patient T16*; left temporal lobe resection anterior to the vein of Labbé (VL); local anesthesia. Cortical stimulation: A, mouth movement to right; B, tongue tingling; C, speech suppression; D, receptive aphasia. *B*: SEPs to stimulation of the contralateral (——) or ipsilateral (- - -) median nerve.

In the recording of Fig. 8 the craniotomy did not expose all of the hand area, as indicated by the results of cortical stimulation and the small amplitude of the short-latency potentials to contralateral stimulation. However, from the lateral portion of the hand area the contralateral N80–P180 precentral (*location 1*) and P80–N180 postcentral (*location 2*) potentials were recorded. From more medial locations (*3* and *4*) near the CS, the N90–P190 periCS potentials were recorded. From the deep electrode of a transcortical pair located in or near the CS (*location 4* deep), large contralateral and ipsilateral potentials were recorded. They appeared to be polarity-inverted counterparts of the periCS potentials recorded from surface *locations 3* and *4*.

### *Surface recordings from periSylvian cortex*

The human second somatosensory area (SII) is probably located mainly in the upper wall of the Sylvian sulcus (SS) and partly on the lateral surface below sensorimotor cortex (Penfield and Jasper 1954; Woolsey et al. 1979). We did not systematically explore surface cortex in this region, but recordings in unanesthetized patients using widely spaced electrodes provided some results. In 6 of 11 such recordings, either no activity was seen or the potentials appeared to be small versions of SEPs recorded from the hand area of sensorimotor cortex.

In the other five cases focal potentials in the periSylvian region were recorded near the junction of the CS and SS. In the patient summarized in Fig. 9, a positivity at ~100 ms (P100) was recorded above the SS (*location 3*), whereas below it (*location 5*) a negativity at about the same latency (N100) was recorded. A later negative-positive sequence (N125 and P200) was seen at all periSylvian locations but was largest at temporal sites (*5* and *6*) near the SS. These potentials were probably not volume conducted from the hand area of sensorimotor cortex because long-latency potentials were small in that region (*locations 1* and *2*) despite the presence of large short-latency potentials. Figure 10 shows similar results. Contralateral stimulation evoked several short-latency potentials, which were small (<10 μV), showed low spatial gradients, and may not have been locally generated. This was the only periSylvian recording in which any evidence of short-latency activity was seen. P100 was recorded above the SS (*location 1*), and N100 was seen at about the same latency below the SS (e.g., *location 5*). This activity was followed by N125–P200, which was large near the SS but showed no consistent change across it. Ipsilateral stimulation evoked potentials of somewhat similar waveform but of longer latency. Similar activity was seen in the other three cases, in one of which potentials at ~185 ms were recorded, positive below the SS and negative above it.

## DISCUSSION

Before discussing the results, three limitations of these intraoperative recordings should be noted. First, long-latency SEPs may be sensitive to the analgesic and anesthetic agents used (Abrahamian et al. 1963; Clark and Rosner 1973; Grundy 1983). In a few patients in whom scalp recordings were obtained from the nonoperated hemisphere before and during surgery, we found that long-latency SEPs were reduced in amplitude and increased in latency under local or general anesthesia. Second, other intraoperative conditions such as brain cooling may also affect SEPs (Allison et al. 1989). Third, time constraints prevented systematic recording from the entire region of exposed cortex. Thus these recordings probably yield an incomplete sample of long-latency cortical activity evoked by median nerve stimuli.

### *Potentials recorded from contralateral sensorimotor cortex*

Despite the limitations noted above, several features of these potentials were reliable enough within and between patients to suggest a consistent pattern of activation of sensorimotor cortex.

In the preceding paper (Allison et al. 1989) we concluded that P20–N30 and N20–P30 are generated in *area 3b* of somatosensory cortex. Results supporting the same conclusion for the P45-N80-P180 precentral and N45-P80-N180 postcentral potentials may be summarized as follows:

*1.* The precentral and postcentral potentials have cortical surface distributions similar to those of P20–N30 and N20–P30, respectively (Figs. 2, 4, and 5).

*2.* There is no evidence of generation of the precentral and postcentral potentials in parietal surface cortex or in motor cortex: a) Transcortical locations across the supramarginal gyrus (Fig. 7, *locations 6* surface and deep) recorded similar P80–N180 potentials from surface and white matter, suggesting that they are not generated in parietal surface cortex. b) Recordings across the anterior wall of the CS showed similar N80–P180 potentials at surface and deep locations (Fig. 7, *locations 2* surface and *3* deep), suggesting that they are not generated in motor cortex.

*3.* Recordings across the posterior wall of the CS (Fig. 7, *locations 3* deep and *4* deep) showed a clear polarity inversion of P45–N45, and less clear inversion of N80–P80 and P180–N180, suggesting their origin in *area 3b*.

N80–P180 and P80–N180 correspond to neuromagnetic peaks in the same latency ranges (Hari et al. 1984; Kaufman et al. 1981). These groups attributed this activity to a tangentially oriented generator in somatosensory cortex.

In the preceding paper (Allison et al. 1989) we concluded that P25–N35 is generated in *area 1* of somatosensory cortex. Results supporting the same conclusion for the P50-N90-P190 periCS potentials may be summarized as follows:

*1.* The periCS potentials often had cortical surface distributions similar to those of P25–N35; they were usually largest over the anteromedial portion of somatosensory cortex near the CS and did not show polarity inversion across it (Figs. 3–5). However, the periCS potentials were often recorded from more lateral regions of the hand area of cortex (Figs. 3 and 4; Fig. 5*C* at 100 ms). In this respect their topography resembled that of the P25-like potentials (Allison et al. 1989), suggesting that various regions of the hand representation of *area 1* respond to median nerve stimuli at some latency. The data are not sufficient to suggest a mediolateral sequence of activation of separate regions of *area 1*, as appears to be the case in the 25 to 40-ms latency range (Allison et al. 1989).

*2.* Transcortical recordings of the periCS potentials were obtained in one case. N90–P190 was recorded close to and on either side of the CS (Fig. 8, *locations 3* surface and *4* surface). From a deep electrode (*location 4*) an apparent polarity inversion was recorded, suggesting that the potentials may have originated in *area 1*.

Additional evidence that these potentials are generated in *area 1* comes from the transcortical recordings of Goldring and colleagues (1970) and Stohr and Goldring (1969). From locations in somatosensory cortex near the CS, they recorded a sequence of potentials very similar in latency and waveform to the P50-N90-P190 periCS potentials, with polarity inversion from surface to white matter. The potentials were consistently recorded from the anterior crown of somatosensory cortex and were occasionally recorded with smaller amplitude and less clear polarity inversion from the crown of motor cortex. Their results thus provide strong evidence that the periCS potentials are generated in *area 1* and possibly to a lesser extent in *area 4*. This may be related to the finding that there is relatively more precentral RMS voltage in the 40 to 108-ms latency range compared with the 20 to 40-ms latency range (cf. Fig. 1 of this paper with Fig. 7 of Wood et al. 1988).

In the preceding paper (Allison et al. 1989) we postulated that generators in *areas 3b* and *1* could account satisfactorily for the short-latency SEPs recorded from sensorimotor cortex. Similar conclusions can be drawn for the long-latency SEPs described here. Specifically, we conclude that *area 3b* generates the P20-N30-P45-N80-P180 sequence of precentral potentials and the N20-P30-N45-P80-N180 sequence of postcentral potentials and that *area 1* generates the P25-N35-P50-N90-P190 sequence of periCS potentials. These conclusions are summarized schematically in Fig. 11, *A* and *B*. The top two waveforms of Fig. 11*B* are postulated generator timecourses of activation of *areas 3b* and *1*. The vertical and horizontal lines in Fig. 11*A* indicate the regions where the largest precentral and postcentral potentials are recorded, whereas the stippling indicates the region of largest periCS potentials. Mixtures of the two types of activity are more likely to be recorded from the region of overlap near the CS, whereas from the nonoverlapped regions relatively distant from the CS, the precentral and postcentral potentials are more likely to be recorded in relative isolation. Because of the vertical orientation of *area 3b*, the precentral and postcentral potentials are recordings from the "surface" and "white matter" sides, respectively, of the tangentially oriented generator. Because of the approximately horizontal orientation of *area 1*, only the surface potentials are seen in cortical surface recordings; the corresponding polarity-inverted white matter potentials can be recorded transcortically as noted above. As was postulated to be the case for short-latency SEPs, the slightly later activation of the *area 1* sequence of potentials compared to the *area 3b* potentials may be because of the smaller size and number of afferent fibers to *area 1* compared with those to *area 3b* (Allison et al. 1989; Jones and Powell 1970). The recording conditions of this study may have biased the results in favor of potentials generated in *areas 3b* and *1*, as discussed in the preceding paper. However, there is weak evidence (Figs. 6 and 7) that long-latency SEPs may also be generated in one or both walls of the PoCS in *areas 2* and *7*.

The neurophysiological events underlying these SEPs can be inferred by comparison with recordings in monkeys. Three studies of SEPs recorded simultaneously with single- or multiple-unit activity have been carried out in sensorimotor cortex of monkeys to electrical stimulation of the median nerve or tactile stimulation of the hand (Arezzo et al. 1981; Gardner et al. 1984; Kulics and Cauller 1986). The potentials recorded in all studies were similar. Correspondences between monkey and human short-latency potentials were discussed in the preceding paper. The monkey potentials relevant to this paper are P20 in the nomenclature of Arezzo et al. (1981), P25 of Gardner et al. (1984), and P1a of Kulics and Cauller (1986); N45 (N43, N1); and P110 (P70, P2). These potentials are best recorded from *area 1* and do not change polarity across the CS; thus they probably correspond to the human periCS potentials P50, N90, and P190 respectively. The monkey P20, corresponding to the human P50, is associated with an increase in unit discharge in *areas 3b, 1*, and *2* of somatosensory cortex and also in *area 5*, and probably reflects the excitation of pyramidal cells. The neurophysiological basis of the monkey N45, corresponding to the human N90, is unclear. Arezzo et al. (1981) and Kulics and Cauller (1986) recorded unit discharges associated with N45 and concluded

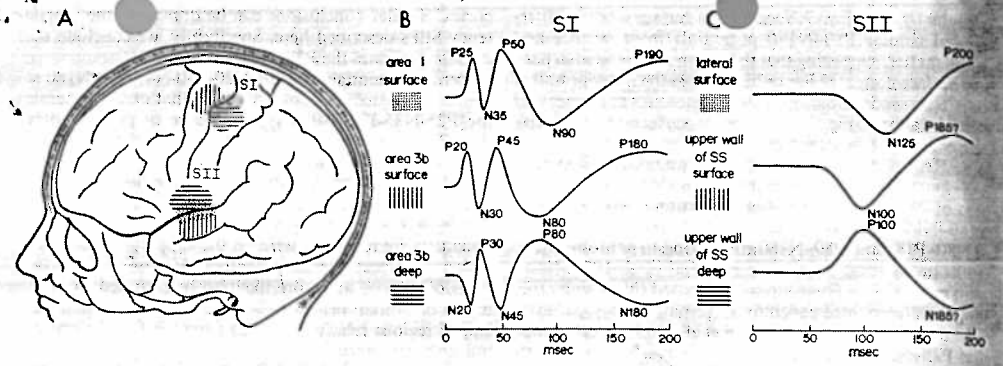


FIG. 11. Postulated SEPs evoked by stimulation of the contralateral median nerve. *A*: regions of surface cortex from which SEPs generated in sensorimotor cortex (SI) and in the second somatosensory area (SII) are recorded, as described in this and the preceding paper (Allison et al. 1989). *B: Area 3b* in the posterior wall of the CS generates the primary positive-negative potentials P20–N30 (*middle*) from the surface of *area 3b* and hence from recording locations anterior to the CS, followed by the P45-N80-P180 precentral potentials. Posterior to the CS, N20–P30 is followed by the N45-P80-N180 postcentral potentials (*bottom*); they are polarity-inverted counterparts of the precentral potentials due to the tangential orientation of the *area 3b* generator. Precentral and postcentral potentials are best recorded respectively from the vertically and horizontally striped regions in *A*. Slightly later, a similar sequence of events, P25–N35 followed by the P50-N90-P190 periCS potentials (*top*), is generated in *area 1* and is best recorded from the stippled region in *A*. This generator is approximately radial, thus its polarity-inverted white matter potentials are not recorded from the cortical surface. *C*: portion of SII in the upper wall of the SS is postulated to generate N100–P185, best recorded from the vertically striped region in *A*. Because of the tangential orientation of this generator, the polarity-inverted "white matter" potentials are recorded as P100–N185 from the horizontally striped region in *A*. Portion of SII in surface cortex above the SS is postulated to generate N125–P200, best recorded from the stippled region in *A*; this generator is approximately radial and its polarity-inverted potentials are not seen in surface recordings.

that it reflects excitatory postsynaptic potentials in somatosensory cortex neurons. However, Gardner et al. (1984) found that N45 was associated with a period of decreased unit activity and concluded that it reflects an inhibitory process. The monkey P110, corresponding to the human P190, appears to be generated in various areas of somatosensory and parietal cortex, but its relationship to unit activity is not sufficiently strong to suggest its neuronal substrate. Unit discharges in *area 3b* were similar to those obtained from *areas 1* and *2*. It is therefore reasonable to conclude that corresponding periCS and precentral potentials (P50 and P45, N90 and N80, and P190 and P180, respectively) reflect similar neuronal events. In none of the monkey studies were unit discharges recorded from motor cortex in the latency range of interest here.

### *Potentials recorded from ipsilateral sensorimotor cortex*

Short-latency SEPs were evoked only by contralateral stimulation (Allison et al. 1989). However, beginning in the 40 to 50-ms latency range, focal potentials of apparent local origin in sensorimotor and parietal cortex were recorded to stimulation of the ipsilateral median nerve in ~40% of the patients so tested. The topography of ipsilateral activity differed from that of contralateral activity. Ipsilateral potentials were not seen which polarity inverted across the CS and thus could be ascribed to activity in *area 3b*. Rather the ipsilateral potentials appeared to arise in a diffuse region of sensorimotor cortex including motor cortex (*area 4*), the crown of the postcentral gyrus (*areas 1* and *2*), and cortex within the walls of the PoCS (*areas 2* and *7*). Most neurons in somatosensory cortex respond only to contralateral stimulation, although in cats some neurons in the lower cortical layers respond to ipsilateral stimulation as well (Towe et al. 1964). These neurons respond later and contribute negligibly to the early potentials recorded at the cortical surface, results consistent with our recordings. However, these neurons are located in the same region in which the largest contralateral potentials are evoked and would thus be expected to evoke topographically similar potentials. The paucity of interhemispheric callosal input to *area 3b* in primates (Killackey et al. 1983) suggests that human ipsilateral potentials are generated by transcallosal input from the contralateral hemisphere in regions of sensorimotor cortex that receive stronger callosal projections and provides a plausible explanation for our failure, and the failure of neuromagnetic recordings (Hari et al. 1984; Kaufman et al. 1981), to record ipsilateral potentials attributable to a generator in *area 3b*.

The initial excitation of non-*area 3b* sensorimotor cortex neurons by a median nerve volley occurs at ~25 ms (judging by the latency of P25), and the onset latency of ipsilateral potentials is ~45 ms (Figs. 6–8), yielding a callosal transmission time of ~20 ms. The interhemispheric conduction distance between the sensorimotor hand areas is ~12 cm (Talairach and Szikla 1967). Callosal conduction velocity is thus ~6 m/s, within the range of conduction velocities (1–10 m/s) estimated for cat somatosensory callosal axons (Miller 1975). Scalp recordings of human SEPs yielded estimated callosal transmission times of 3–8 ms (Salamy 1978), but this is likely an underestimate given the distribution of callosal axon diameters (Innocenti 1986; Swadlow et al. 1979).



### *Potentials recorded from periSylvian cortex*

In monkeys SII is located within the upper wall of the lateral sulcus (Robinson and Burton 1980a), corresponding to the human SS. Data concerning the exact location and functional organization of SII in man are scant. The results of cortical stimulation suggest that SII is located partly in the upper wall of the SS and partly in surface cortex above the SS and below the face area of sensorimotor cortex (Penfield and Jasper 1954). From the latter region, foot movement to cortical stimulation and SEPs to stimulation of the contralateral thumb were obtained in one patient (Woolsey et al. 1979). Thus there is some evidence that the human SII is partially located on the lateral surface of cortex above the SS as well as in its upper wall, corresponding to portions of *areas 40* and *43*. Median nerve SEPs in the vicinity of the SS might reflect potentials generated in SII, particularly because much of this region is devoted to representation of the hand (Robinson and Burton 1980a).

Our recordings provide preliminary evidence of potentials in the 100-ms latency range that invert in polarity across the SS and thus may reflect activity generated in the upper wall of the SS. These potentials probably reflect the same activity as the 100-ms peak seen in neuromagnetic recordings in humans and ascribed to a generator in SII (Hari et al. 1984). The N100–P100 potentials recorded from the periSylvian region may be neurophysiologically similar to the N80–P80 potentials recorded from sensorimotor cortex; in both cases the potential field is negative on the surface side of cortex (and hence negative over temporal and frontal cortex, respectively) and positive deep to cortex (and hence positive over the frontoparietal operculum and parietal cortex, respectively). The N125 and P200 potentials did not change across the SS and may be generated in the portion of SII located on the lateral surface above the SS. They may be neurophysiologically similar to the N90 and P190 potentials recorded from sensorimotor cortex.

The postulated periSylvian potentials and the regions from which they are recorded are summarized schematically in Fig. 11, *A* and *C*. This summary is based on few recordings and is presented only as a working hypothesis. The 100-ms activity was seen consistently in our recordings and in neuromagnetic recordings (Hari et al. 1984), but the proposed 185-ms activity was seen in only one of our recordings and was not consistently seen in neuromagnetic recordings (Hari et al. 1984). The 125- and 200-ms activity was seen consistently in our recordings but was not observed in neuromagnetic recordings (Hari et al. 1984), perhaps because it is due to an approximately radial generator in lateral cortex, to which neuromagnetic recordings are insensitive. Animal recordings (e.g., Andersson 1962) suggest that short-latency SEPs should be generated in human SII, but if so they have not been detected in our recordings or in magnetic recordings (Hari et al. 1984). The periSylvian potentials were evoked by both ipsilateral and contralateral stimulation in the one patient in whom both median nerves were stimulated (Fig. 10). This suggests a generator in SII, because ~20% of neurons in the hand representation of SII receive ipsilateral input (Robinson and Burton 1980a). It is possible that the periSylvian potentials are generated partly in the temporal lobe, but in monkeys few neurons in the temporal lobe near the SS are responsive to somatosensory stimuli (Baylis et al. 1987). Generators in SII proper or in nearby regions of the parietal operculum that also respond to somatosensory stimuli (Robinson and Burton 1980b) seem more likely.

We thank R. Bartozzi, J. Jasiorkowski, M. Pearson, E. Roessler, and D. Thompson for assistance. Drs. R. Bucholz, P. Dickey, J. Partington, J. Piepmeier, and J. C. VanGilder collaborated in some recordings, and Drs. S. J. Jones and J. Wolpaw provided helpful reviews of previous versions of this paper.

This work was supported by the Veterans Administration and by National Institute of Mental Health Grant MH-05286.

Address for reprint requests: T. Allison, Neuropsychology Laboratory 116B1, V.A. Medical Center, West Haven, CT 06516.

Received 25 April 1988; accepted in final form 27 April 1989.

## REFERENCES

ABRAHAMIAN, H. A., ALLISON, T., GOFF, W. R., AND ROSNER, B. S. Effects of thiopental on human cerebral evoked responses. *Anesthesiology* 24: 650–657, 1963.

ALLISON, T., MCCARTHY, G., WOOD, C. C., DARCEY, T. M., SPENCER, D. D., AND WILLIAMSON, P. D. Human cortical potentials evoked by stimulation of the median nerve. I. Cytoarchitectonic areas generating short-latency activity. *J. Neurophysiol.* 62: 694–710, 1989.

ANDERSSON, S. A. Projection of different spinal pathways to the second somatic sensory area in cat. *Acta Physiol. Scand.* 56, *Suppl.* 194: 1–74, 1962.

AREZZO, J. C., VAUGHAN, H. G., JR., AND LEGATT, A. D. Topography and intracranial sources of somatosensory evoked potentials in the monkey. II. Cortical components. *Electroencephalogr. Clin. Neurophysiol.* 51: 1–18, 1981.

BAYLIS, G. C., ROLLS, E. T., AND LEONARD, C. M. Functional subdivisions of the temporal lobe neocortex. *J. Neurosci.* 7: 330–342, 1987.

CLARK, D. L. AND ROSNER, B. S. Neurophysiologic effects of general anesthetics: I. The electroencephalogram and sensory evoked responses in man. *Anesthesiology* 38: 564–582, 1973.

GARDNER, E. P., HÄMÄLÄINEN, H. A., WARREN, S., DAVIS, J., AND YOUNG, W. Somatosensory evoked potentials (SEPs) and cortical single unit responses elicited by mechanical tactile stimuli in awake monkeys. *Electroencephalogr. Clin. Neurophysiol.* 58: 537–552, 1984.

GOLDRING, S., ARAS, E., AND WEBER, P. C. Comparative study of sensory input to motor cortex in animals and man. *Electroencephalogr. Clin. Neurophysiol.* 29: 537–550, 1970.

GRUNDY, B. L. Intraoperative monitoring of sensory-evoked potentials. *Anesthesiology* 58: 72–87, 1983.

HARI, R., REINIKAINEN, K., KAUKORANTA, E., HÄMÄLÄINEN, M., ILMONIEMI, R., PENTTINEN, A., SALMINEN, J., AND TESZNER, D. Somatosensory evoked cerebral magnetic fields from SI and SII in man. *Electroencephalogr. Clin. Neurophysiol.* 57: 254–263, 1984.

INNOCENTI, G. M. General organization of callosal connections in the cerebral cortex. In: *Cerebral Cortex. Sensory-Motor Areas and Aspects of Cortical Connectivity*, edited by E. G. Jones and A. Peters. New York: Plenum, 1986, vol. 5, p. 291–353.

JONES, E. G. AND POWELL, T. P. S. Connexions of the somatic sensory cortex of the rhesus monkey. III. Thalamic connexions. *Brain* 93: 37–56, 1970.

KAUFMAN, L., OKADA, Y., BRENNER, D., AND WILLIAMSON, S. J. On the relation between somatic evoked potentials and fields. *Int. J. Neurosci.* 15: 223–239, 1981.

KILLACKEY, H. P., GOULD, H. J., III, CUSICK, C. G., PONS, T. P., AND KAAS, J. H. The relation of corpus callosum connections to architectonic fields and body surface maps in sensorimotor cortex of new and old world monkeys. *J. Comp. Neurol.* 219: 384–419, 1983.

KULICS, A. T. AND CAULLER, L. J. Cerebral cortical somatosensory evoked responses, multiple unit activity and current source-densities: their interrelationships and significance to somatic sensation as revealed by stimulation of the awake monkey's hand. *Exp. Brain Res.* 62: 46–60, 1986.

MILLER, R. Distribution and properties of commissural and other neurons in cat sensorimotor cortex. *J. Comp. Neurol.* 164: 361–374, 1975.

PENFIELD, W. AND JASPER, H. *Epilepsy and the Functional Anatomy of the Human Brain.* Boston, MA: Little, Brown, 1954.

ROBINSON, C. J. AND BURTON, H. Somatotopographic organization in the second somatosensory area of *M. fascicularis. J. Comp. Neurol.* 192: 43–67, 1980a.

ROBINSON, C. J. AND BURTON, H. Organization of somatosensory receptive fields in cortical areas 7b, retroinsula, postauditory and granular insula of *M. fascicularis. J. Comp. Neurol.* 192: 69–92, 1980b.

SALAMY, A. Commissural transmission: maturational changes in humans. *Science Wash. DC* 200: 1409–1411, 1978.

STOHR, P. E. AND GOLDRING, S. Origin of somatosensory evoked scalp responses in man. *J. Neurosurg.* 31: 117–127, 1969.

SWADLOW, H. A., GESCHWIND, N., AND WAXMAN, S. G. Commissural transmission in humans. *Science Wash. DC* 204: 530–531, 1979.

TALAIRACH, J. AND SZIKLA, G. *Atlas of Stereotaxic Anatomy of the Telencephalon.* Paris: Masson, 1967.

TOWE, A. L., PATTON, H. D., AND KENNEDY, T. T. Response properties of neurons in the pericruciate cortex of the cat following electrical stimulation of the appendages. *Exp. Neurol.* 19: 325–344, 1964.

WOOD, C. C., SPENCER, D. D., ALLISON, T., MCCARTHY, G., WILLIAMSON, P. D., AND GOFF, W. R. Localization of human sensorimotor cortex during surgery by cortical surface recordings of somatosensory evoked potentials. *J. Neurosurg.* 68: 99–111, 1988.

WOOLSEY, C. N., ERICKSON, T. C., AND GILSON, W. E. Localization in somatic sensory and motor areas of human cerebral cortex as determined by direct recording of evoked potentials and electrical stimulation. *J. Neurosurg.* 51: 476–506, 1979.

JOURNAL OF NEUROPHYSIOLOGY
Vol. 62, No. 3, September 1989. *Printed in U.S.A.*

# Classification of Turtle Retinal Ganglion Cells

A. M. GRANDA AND J. E. FULBROOK
*Program in Neuroscience, School of Life and Health Sciences, University of Delaware, Newark, Delaware 19716*

## SUMMARY AND CONCLUSIONS

*1.* Receptive fields of 78 retinal ganglion cells were analyzed for their responses to moving and stationary lights that were presented under a variety of stimulus conditions. All cells were sensitive to moving stimuli, and their receptive fields often comprised excitatory and inhibitory sub-regions.

*2.* Properties used in the classification included responses to stationary flashed stimuli, receptive-field organization, changes in stimulus wavelength and adaptation, movement velocity, and direction of stimulus movement. Eight functional cell classes were derived: simple, ON-sustained, annular, wavelength-sensitive, directionally selective, bar-shaped, large-field, and velocity.

*3.* Simple cells, representing 21% of the sample, had circular or oval receptive fields of 3–22° that gave transient responses to stationary, flashed lights. Many of these cells, but not all, showed antagonistic center-surround organizations. ON-sustained cells responded for the duration of the stimulus flash or for the duration of a light flash moving through the receptive field. These units comprised 8% of the sample; they had small, circular, nondirectional receptive fields and they were most sensitive to red light. Their field sizes did not vary with changes in adaptation level.

*4.* Annular cells (4% of the sample) gave no responses to any stimulation in the field center, but they responded strongly to stimulation in the surround area, especially to stimuli that moved very slowly through the region. Annular cells were nondirectional, with circular centers of 5–6° diam and annular surround widths of 2–4°. They responded best in light adaptation.

*5.* Wavelength-sensitive cells, similar to most of the cells sampled, were sensitive to red light when light-adapted. Some cells in addition showed input from rods under dark adaptation. Intensity-response curves for these latter cells showed clear changes from one input to the other as the cells' functional ranges were explored. Some cells responded best to short- or middle-wavelength light, but these were more rarely met. Where multiple receptor inputs could be identified, long-wavelength stimuli evoked transient responses, whereas short-wavelength stimuli favored more sustained spike trains. Wavelength-sensitive cells in this category comprised 5% of the sample.

*6.* Directionally selective cells had both circular and elongated receptive fields, the latter oriented orthogonally to their preferred-null axes. This group, made up of ON, OFF, and ON-OFF cells, comprised 23% of the recorded sample. When combined with seven bar-shaped cells and one large-field cell that were also directionally selective, the sample yielded a total of 31 out of 78 recorded cells, or 40%, the highest proportion of directionally selective ganglion cells reported in the literature. The ON cells differed from other directionally selective cells by requiring large, bright, slow-moving stimuli. These cells also gave robust OFF responses to light spots as they left the receptive field in the null direction; OFF and ON-OFF cells gave no responses at all under these conditions.

*7.* Bar-shaped cells had length-to-width ratios in the range of 2:1–10:1. These cells comprised 12% of the population and were distributed into four cell sub-categories: single-bar, directionally selective, OFF cells; single-bar, bidirectional, ON cells; double-bar, directionally selective, ON-OFF cells; and triple-bar, bidirectional, ON and OFF cells.

*8.* Large-field cells (6% of the sample) had enormous field lengths of ≥25°. Some fields were crescent-shaped to an extent of 75°. In general, these cells were nondirectional and preferred slow-moving targets. They showed no appreciable changes in field size to changes in stimulus wavelength or to adaptation.

*9.* Velocity cells responded better to targets moving at speeds >9°/s, with few or no responses at slower speeds. Fifteen percent of the sample fell into this class. All cells had circular or oval receptive fields, were red-light sensitive, and gave ON-OFF responses to stationary, flashed stimuli; all were nondirectional.

*10.* Retinal ganglion cells in turtle are exceedingly complex. Their response properties can be manipulated by changes in stimulus parameters. In the number and variety of retinal ganglion cell types, turtles possess one of the more sophisticated response repertoires recognized at that level in vertebrates.

## INTRODUCTION

The morphological diversity of ganglion cells has always supposed a parallel functional complexity, and in turtles where ganglion cell polymorphism is particularly profuse (Cajal 1892; Kolb 1982), there is natural curiosity as to what their functional properties might be.

It was Lipetz and Hill (1970) who first classified ganglion cell responses in the turtle *Emys blandingii*, and found the cells to be sensitive to stimulus movement—many cells responding best at particular velocities, some cells responding maximally in preferred directions. The receptive fields they described were either circular or oval, and reflected all three response types described by Hartline (1938), viz., ON, OFF, and ON-OFF. Bowling (1980), in a later study, grouped ganglion cells of *Pseudemys* into four categories: motion-sensitive cells, directionally selective cells, color cells, and orientation cells. Most of the cells he reported on were red-light sensitive, with a majority of these also sensitive to input from rods. Granda and Fulbrook (1982) soon after were able to show complicated effects within the receptive fields with regard to color, adaptation, and movement, as well as a diversity of receptive-field arrangements. In several experiments based on intracellular recordings, Marchiafava and co-workers (1980, 1981, 1983) described two classes of ganglion cells defined by their inputs from either bipolar cells alone (Type A), with an emphasis on color opponency, or from mixed inputs from bipolar and amacrine cells (Type B), with a peak sensitivity of 646 nm in both the center and the surround of the receptive field. Type A cells were found to have faster conduction velocities than Type B cells.